Evaluating Finite Element Analysis for Shaped Charge Dynamics: A Study of 2D and 3D Simulations Using ABAQUS.

OWEN MILLER

BAE SYSTEMS, UNIVERSITY OF WALES TRINITY ST DAVID

04/01/2025

I. Abstract

This report investigates the application of Finite Element Analysis (FEA) for modelling the dynamics of shaped charges, with a focus on the capabilities and limitations of ABAQUS software. Shaped charges are explosive devices designed to produce high-velocity jets capable of penetrating dense materials, with the performance influenced by factors such as charge geometry, liner material, and explosive properties. Both 2D and 3D simulations were conducted to evaluate jet formation, pressure wave propagation, and material deformation, with results validated against theoretical models and literature.

The 2D simulations demonstrated strong alignment with established theories, including the Gurney and Pugh-Eichelberger-Rostoker (PER) models, accurately replicating jet velocities and collapse dynamics while maintaining computational efficiency. In contrast, 3D simulations introduced significant challenges, such as increased element counts, node overstretching, and deviations in pressure wave behaviour, leading to discrepancies in jet formation and velocity. Adaptive meshing was implemented to improve stability in 3D modelling, extending simulation durations and reducing failure rates, but anomalies in energy transfer and nodal interactions remained.

The findings emphasise the effectiveness of 2D simulations for shaped charge design, offering reliable insights with significantly lower computational demands compared to 3D. While 3D modelling can provide additional details, its increased complexity often outweighs the benefits for most practical applications. The study concludes that FEA should be integrated with validated literature and live testing to ensure accurate and safe

shaped charge designs. By highlighting the strengths and limitations of ABAQUS, this report establishes a framework for leveraging FEA as a complementary tool in the development and assessment of shaped charges.

II. Table of Figures

Figure No	Figure
1	Shape charge configuration + geometric parameters
2	ABAQUS Charge 1 Drawing dimensions
3	Charge 1 Assembly
4	final time step Tri Node, step time 9.8418e-05s
5	final time step Tet Node, Step time 6.3837e-05s
6	use of local and general seeding
7	– jet formation of 0.004 Seeded / 0.008 general Mesh
8	jet formation of 0.002 Seeded / 0.004 general Mesh
9	jet formation of 0.001 Seeded / 0.002 general Mesh
10	Literature Jet formation at 6.9e-5s
11	Charge 1 Jet formation at 6.9e-5s
12	Velocity over time literature charge
13	Velocity over time charge 1
14	Jet Tip formation zone
15	charge 1 jet tip formation elements
16	pressure wave propagation in charge 1
17	120-degree cone angle Shaped Charge
18	charge 2 deformation
19	charge 2 jet tip velocity
20	Pressure wave formation charge 2
21	Charge 3 parts
22	Charge 3 Assembly
23	Charge 3 Mesh validation
24	initial liner Reaction, final time step
25	SPH shape charge visualisation
26	Area for Adaptive Meshing + full run with secondary parameters
27	Initial linear and quadratic viscosity parameters
28	adapted linear and quadratic viscosity parameters
29	Frequency of remeshing sweeps
30	Weight values
31	Charge 3 final jet formation
32	Material deformation in jet formation
33	Pressure wave propagation in HE, 3D
34	Charge 3 jet tip velocity

III. Table of Tables

Table No	Table
1	Copper Liner material Properties
2	TNT Material Properties
3	Aluminium Case Material Properties
4	Meshing Results

IV. Table of Contents

I. Abstract 2

II. Table of Figures 4

III. Table of Tables 5

IV. Table of Contents 6

1. Introduction 8

2. Literature Review 9

2.1. Background on Shaped Charges 9

2.2. Cone Angle 10

2.3. Liner Material 12

2.4. Numerical and experimental validation 12

2.5. Comparison of FEA Tools for Shaped Charge Analysis 13

2.6. Assumptions and validation 15

3. 2D Validation and Analysis of Shaped Charges 17

3.1. 2D Modelling validation compared with literature 17

3.2. Jet formation theory 36

3.3. Pressure wave propagation 38

3.4. Validation Summary 38

4. 2D Shape charge with 120-degree Apex angle and Radius 39

4.1. Liner Deformation 41

4.2. Jet tip Velocity 42

4.3. Pressure wave formation 43

4.4. Overall 43

5. 3D modelling of charge 2 44

5.1. Initial results 47

5.2. Final adaption results 52

6. Discussion 55

6.1. 2D vs. 3D Simulations 55

6.2. Expected and Unexpected Results 56

6.3. Interpretation and comparison with theory 57

6.4. Generality and future Implications 57

7. Conclusion 58

8. Bibliography 59

1. Introduction

Shaped charges are explosive devices designed to concentrate detonation energy into a high-velocity jet, enabling the penetration of dense materials. The effectiveness of these devices is determined by various factors, including the charge geometry, liner material, and explosive properties. Understanding these variables is critical for optimising shaped charge performance and ensuring reliability and safety in practical applications.

Finite Element Analysis (FEA) provides a powerful computational approach for modelling shaped charge dynamics, allowing researchers to simulate jet formation, pressure wave propagation, and material deformation under controlled conditions. By reducing the reliance on physical prototypes, FEA offers a time-effective and safer alternative for preliminary analysis. However, the accuracy of FEA simulations depends on validation against established theoretical models and experimental findings, as discrepancies can arise from computational constraints, assumptions, or inaccuracies in the material behaviour modelling.

This report evaluates the use of ABAQUS as an FEA tool for shaped charge analysis, focusing on its ability to simulate key behaviours and validate results against literature benchmarks. The study explores the transition from 2D to 3D modelling, highlighting the challenges and limitations associated with increased complexity and computational demands. Through this analysis, the report aims to assess the reliability of FEA in predicting shaped charge performance and its role as a precursor to live testing.

2. Literature Review

2.1. Background on Shaped Charges

2.1.1. Shaped charges are explosive devices designed to concentrate detonation energy through a cavity to produce a high-velocity jet capable of penetrating dense materials. Performance depends on the geometry of the charge, the material properties of the liner, and the characteristics of the explosive [1].

2.1.2. The operation of shaped charges is explained by fundamental theories, including the Gurney and Pugh-Eichelberger-Rostoker (PER) models. The Gurney model describes the distribution of explosive energy and its conversion into the kinetic energy of the jet, while the PER model incorporates unsteady dynamics, accounting for variations in collapse velocity along the liner. These theories are used to predict jet characteristics such as velocity and mass [1].

2.1.3. The Gurney model focuses on the conservation of energy within the system, predicting the initial velocity of the liner based on the ratio of explosive mass to liner mass. The mathematical formula used in Gurney theory is:

$$V = \sqrt{2E\left(\frac{M}{C} + 0.5\right)^{-1/2}}$$

V represents the initial Gurney velocity of the liner, E is the energy of the explosive per unit mass, C is the mass of the explosive material and M is the mass of the liner or casing. The formula assumes that the explosive energy is instantaneously converted into kinetic energy and distributed between the liner

and the detonation products. While effective for simple geometries and uniform materials, this model does not account for dynamic effects or variations in liner behaviour during collapse [2].

2.1.4. The PER model considers the unsteady collapse of the liner and variations in collapse velocity along its length. This model predicts that the velocity of the liner decreases progressively from the apex to the base due to differences in the time and energy distribution of the detonation wave. It introduces variables such as the collapse angle and deflection angle to refine the prediction of jet tip velocity and mass. The PER model is crucial for accurately describing jet formation dynamics in shaped charge designs [3].

2.2. Cone Angle

2.2.1. The cone angle of a shaped charge liner significantly influences the velocity, coherence, and penetration depth of the jet. The angle determines the geometry of the collapse and the energy concentration during detonation, which directly affects the jet's formation and its subsequent behaviour [4].

2.2.2. Smaller cone angles typically produce jets with higher velocities. These jets are ideal for achieving deep penetration into dense materials due to concentrated energy and high speed. However, the narrower jet width limits the damage area, making them less suitable for applications requiring broader apertures.

2.2.3. Larger cone angles produce slower jets with wider diameters. These jets exhibit lower penetration depths but create larger entrance apertures, making them more effective for operations requiring significant target disruption, such as breaching or perforation applications.

2.2.4. Optimal cone angles are often in the range of 40° to 60°, depending on the desired balance between penetration depth and aperture size. Numerical studies have shown that variations in the cone angle lead to distinct velocity profiles along the jet, with smaller angles maximising tip velocity while larger angles enhance jet stability and coherence [4].

2.2.5. In FEA simulations, variations in cone angle result in distinct differences in jet formation and penetration outputs. Smaller cone angles tend to produce higher peak jet velocities in simulations, which aligns with the ability to achieve greater penetration depths. Larger cone angles, however, show greater deformation of the liner and more widespread energy dissipation, which is reflected in simulations as lower jet velocities but larger penetration apertures [5]. FEA also highlights that the collapse dynamics and material flow are more sensitive to mesh density and solver settings when the cone angle is decreased, which can cause consistent failures when 3D modelling [6].

2.3. Liner Material

The choice of material impacts the liner's ability to collapse, form a coherent jet, and maintain its structural integrity during the detonation process.

2.3.1. Malleable materials, such as copper, are commonly used for liners due to high ductility and ability to deform plastically under explosive force. This property allows the material to collapse efficiently and form a continuous, coherent jet with minimal fragmentation. Copper's relatively high density also contributes to the production of high-velocity jets with significant penetration depth [1].

2.3.2. FEA simulations demonstrate that liners made from malleable materials exhibit more predictable collapse dynamics and jet formation. This predictability reduces computational uncertainty [7].

2.4. Numerical and experimental validation

2.4.1. The use of FEA enables researchers to model the collapse of the liner, the jet's velocity distribution, and its interaction with a target (not completed in this example). This approach normally serves as a precursor to physical experimentation, ensuring that a proposed design performs as intended [8].

2.4.2. FEA is used for refining liner designs by predicting the dynamic response of materials under extreme conditions. For example, it allows the analysis of variables such as liner collapse geometry, jet coherence, and velocity profiles

without the immediate need for physical prototypes. This can shorten development cycles, and minimises the risks associated with live firings. In addition, FEA provides insights into the safety performance of a charge, such as the proper functioning of standoff distances and containment systems, ensuring that designs meet operational safety standards [9].

Live firings are essential for validating the results of FEA simulations. Parameters such as jet velocity, penetration depth, and aperture size measured during physical tests are compared against the predictions from numerical models. This iterative process ensures that simulations accurately reflect real-world performance.

2.5.Comparison of FEA Tools for Shaped Charge Analysis

Various FEA software tools are used for simulating shaped charges, including ABAQUS, AUTODYN, and ANSYS. Each has unique strengths depending on the specific requirements of the analysis.

2.5.1. ABAQUS

ABAQUS excels in simulating large deformations and material non-linearities, both of which are critical in modelling the collapse of liners and jet formation. It supports Arbitrary Lagrange-Eulerian (ALE) methods, allowing for accurate modelling of the high-speed material flow typical of shaped charge detonations. ABAQUS also provides advanced material models, such

as Johnson-Cook and Mie-Grüneisen, to handle the high strain rates experienced during detonation. Its adaptive meshing capabilities ensure efficient computations while maintaining precision in regions of high deformation, such as the liner collapse zone [10].

2.5.2. AUTODYN

AUTODYN is known for simulating detonation and shock wave propagation. It provides a material database tailored to explosive simulations and offers workflows for modelling explosive events. While AUTODYN is effective for shock wave analysis, its limited customisation options and interface flexibility make it less adaptable for user-defined scenarios compared to ABAQUS [11].

2.5.3. ANSYS

ANSYS is a general-purpose FEA software that is often used for structural and thermal simulations. While it can be applied to shaped charge analysis, its support for Eulerian and ALE methods is less developed than that of ABAQUS. ANSYS is better suited for problems with less severe deformations, such as structural integrity assessments of the charge casing, but may lack precision in jet formation modelling [12].

2.5.4. Why ABAQUS is Preferred for Shaped Charge Simulations:

- Flexibility and Customisation: ABAQUS offers significant flexibility in defining material behaviours and incorporating custom material properties.
- Coupled Simulations: The ability to couple thermal, structural, and fluid analyses makes ABAQUS particularly suited for modelling the interaction of explosive materials and liners.
- Detailed Output: ABAQUS provides extensive post-processing tools, enabling detailed analysis of jet formation, velocity profiles, and material behaviour during the detonation process.

2.6.Assumptions and validation

2.6.1. Numerical simulations of shaped charges rely on assumptions to simplify the physics of liner collapse, jet formation, and target interaction. These assumptions are essential to reduce computational complexity but must be validated against established findings in literature to ensure accuracy and reliability.

2.6.2. Common Assumptions in Shaped Charge Simulations [13]

- Material Uniformity: Simulations often assume homogeneous material properties for liners and explosives. This simplification disregards real-world imperfections, such as voids or density gradients, which can influence jet behaviour and penetration outcomes.

- Symmetry: Axial symmetry is assumed to minimise computational demands. This assumption holds for well-designed charges but may overlook real-world asymmetries caused by manufacturing deviations or misalignments.
- Ideal Detonation: Detonation is modelled using simplified equations of state, such as the Jones-Wilkins-Lee (JWL) model, which presumes instantaneous energy release and uniform detonation propagation. Real detonation processes may involve localised variations in pressure and energy distribution.
- Boundary Conditions: Simplified boundary conditions are often applied to the charge, jet, and target, neglecting secondary effects such as shock wave reflections, environmental interactions, or target heterogeneities.

2.6.3. Validation Through Literature Comparison

Validation of these numerical models is commonly achieved by comparing simulation results with data from established literature rather than physical experiments. This approach ensures that the models adhere to proven phenomena and provides confidence in predictive capabilities.

2.6.4. Ongoing Refinement Using Literature

Where discrepancies arise between the simulation outputs and literature benchmarks, refinements are introduced into models for example:

- Updating detonation models to reflect more complex energy distributions observed in prior studies (not present in this example).
- Adjusting boundary conditions to replicate the dynamic behaviours documented in literature.

3. 2D Validation and Analysis of Shaped Charges

3.1. 2D Modelling validation compared with literature

3.1.1. The literature investigates shaped charge performance through numerical simulations using the Multi-Materials Arbitrary Lagrangian Eulerian (MMALE) method in LS-DYNA. The focus is on jet formation and penetration capabilities of various liner geometries. Among these, the conical liner served as a baseline due to its widespread use and well-documented performance in producing high-velocity jets. The simulations were carried out using a 2D axial symmetry configuration [14].

The purpose of using this literature is to validate the effectiveness of ABAQUS as a simulation tool by comparing its results with those documented. The literature provides a benchmark due to its representations of jet formation, acceptable jet velocities for the materials used and penetration capabilities (though penetration will not be included in the ABAQUS results for this study).

3.1.1.1. The primary validation focuses will include:

- Jet Visual Formation: Observing the overall jet structure at similar time steps to ensure consistency in collapse dynamics.
- Jet Tip Velocities: Comparing the peak velocities at similar time steps to evaluate the predictive accuracy of ABAQUS against known results.

3.1.1.2. Additional validations will assess:

- Pressure Wave Formations: Examining the propagation and influence of detonation-induced pressure waves on liner collapse.
- Jet Formation Dynamics: Tracking the initial locations and movements of nodes that eventually form the jet tip, ensuring alignment with known physical behaviours.

This approach ensures that ABAQUS can reliably replicate key phenomena observed in shaped charge simulations

3.1.2. Geometric specifications:

- A copper liner with a thickness of 2mm.
- TNT as the explosive fill.
- An aluminium casing of 2mm.
- A stand-off distance of 200 mm was used to evaluate jet formation (the interaction between the jet and target are not necessary for the comparisons made in this report, thus target is ignored).

- A representation of this configuration and full geometric values are outlined in figure 1.
- The full height of the shape charge is assumed to be 3x h.

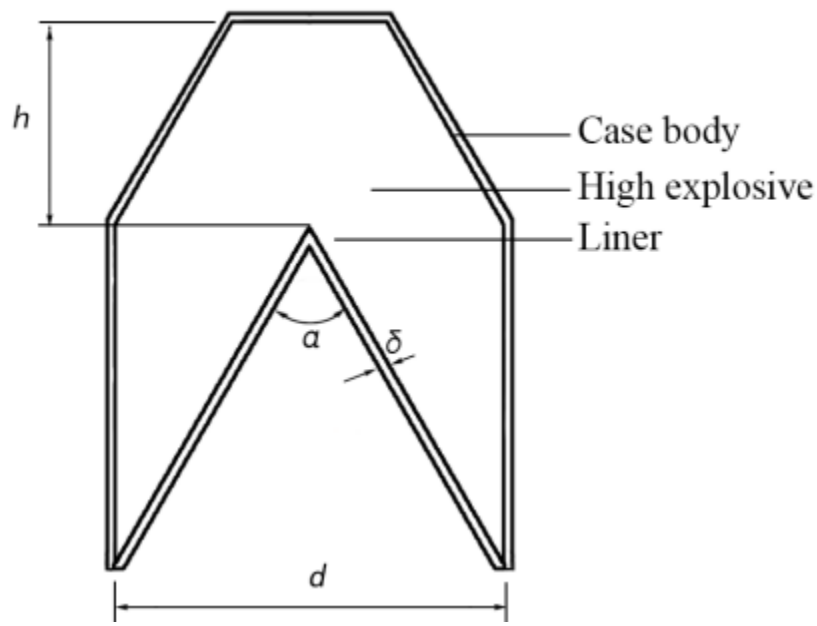

Liner thickness δ(cm)	Height of expl. filling h(cm)	Diameter d(cm)	Apex angle α(°)
0.20	5.29	10.00	60

Figure 1 – shape charge configuration + geometric parameters [14]

3.1.3. Material Specification (note: all properties are from referenced material within [14])

- A copper liner with a thickness of 2mm [15].

Density	
Mass Density	8960kg/m^-3
Elastic	
Shear Modulus	4.6e+10Pa
Eos - Mie–Grüneisen	
c	3940 m/s
s	1.489
Gamma	2

Johnson-Cook Plastic	
A	9e+7Pa
B	2.92e+8Pa
n	0.31
m	1.09
Melting Temperature	1356K
Transition Temperature	288K
Rate Dependant Johnson Cook Hardening	
C	0.025
Epsilon Dot Zero	1

Table 1 – Copper Liner material Properties [15]**.**

- TNT as the explosive fill [17].

Density	
Mass Density	1.7g/cm^-3 [16]
Eos - JWL	
Detonation Wave Speed	8000m/s [16]
A	6.14e+7
B	1.25e+7
Omega	0.25
R1	4.6
R2	1.5
Detonation Energy Density	3.71e+6J/m^3
Pre-Detonation Bulk Modulus	8.92e+9n/m2

Table 2 – TNT Material Properties [17]**.**

- An aluminium casing of 2mm [18].

Density	
Material Density	7870kg/m^-3
Elastic	
Youngs Modulus	6.9e+10Pa
Poisson's Ratio	0.33
Johnson-Cook Plastic	
A	1.1e+8Pa
B	1.5e+8Pa
n	0.36
m	1
Melting Temperature	923K
Transition Temperature	296K
Rate Dependant Johnson Cook Hardening	
C	0.014
Epsilon Dot Zero	1

Table 3 – Aluminium Case Material Properties [18].

3.1.4. Abaqus Validation Charge Design

The Shaped charge was created as per the specification outlined in Figure 1.

(this charge will be referred to as **Charge 1**).

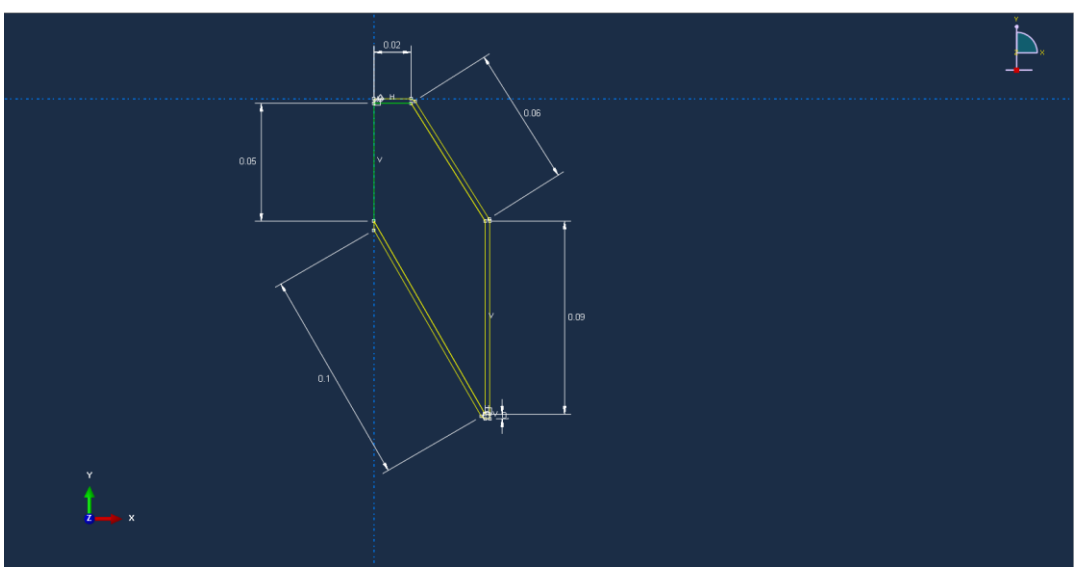

Figure 2 – ABAQUS Charge 1 Drawing dimensions

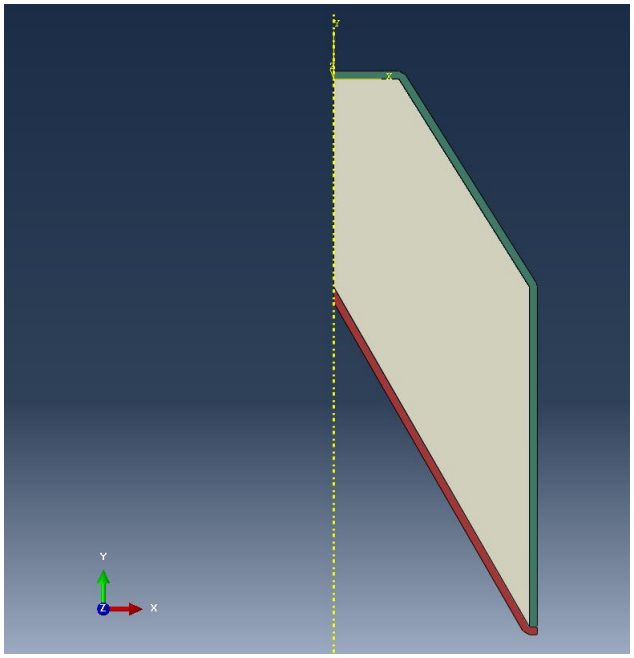

Figure 3 – Charge 1 Assembly

Figure 3 shows the full charge assembly with the green area – aluminium case, beige area – TNT Fill, red area – copper liner.

3.1.5. Charge 1 general validations

Several general validation aspects were addressed based on insights from early simulations and verified external literature.

3.1.5.1. General contact model

The contact model was defined as general (all faces with all touching faces) defining specific contact faces presented no benefit in simulation stability.

3.1.5.2. Element selection: Tri vs Tet

Triangular (tri) elements were selected for simulations due to suitability for handling academic license limitations (node count constraints). Tri elements, with three nodes per element, allow for tighter mesh generation without exceeding the node limit. In contrast, tetrahedral (tet) elements, which are four-sided, require hybrid configurations when interfacing the liner and TNT charge. Hybrid configurations can cause node overexertion, leading to increased likelihood of overlapping between nodal points thus crashing [19].

The use of tri elements also impacted the simulation's final time step. Simulations using tri elements reached a final time step approximately 15% further into the simulations compared to those using tet elements

shown in Figures 4 + 5. This indicates that tri elements provided more stable and efficient meshing.

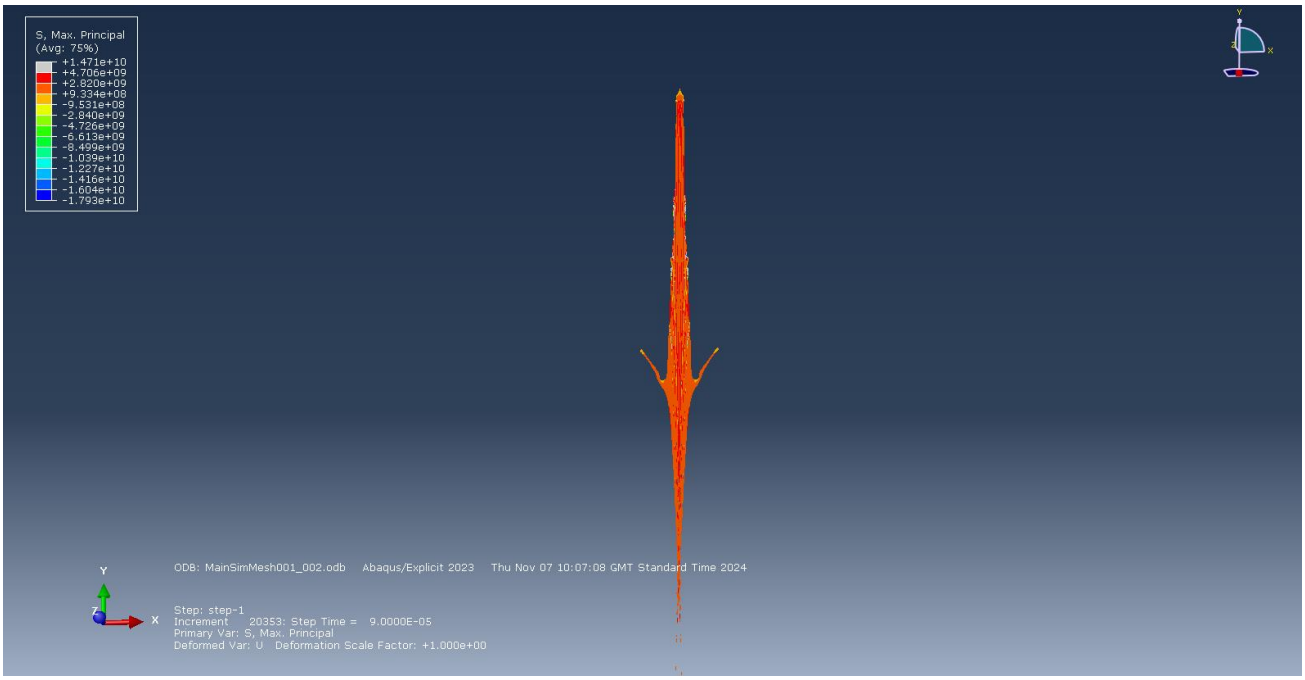

Figure 4 – final time step Tri Node, step time 9.8418e-05s

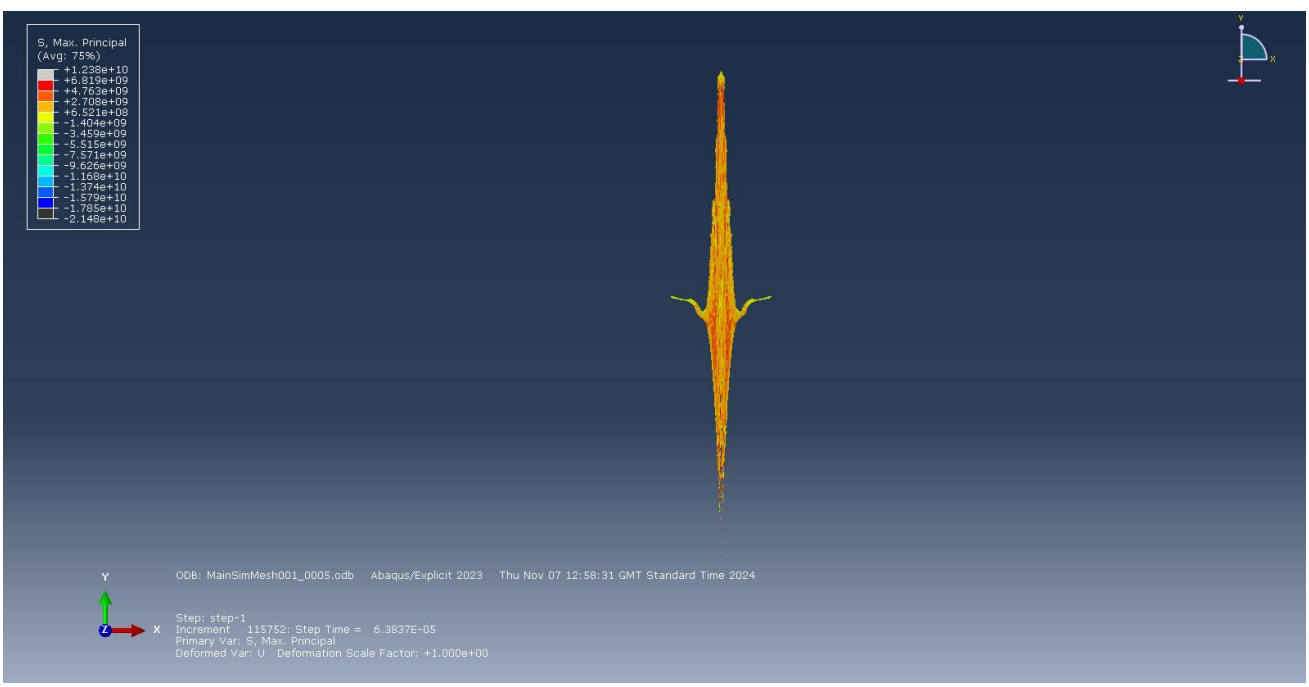

Figure 5 – final time step Tet Node, Step time 6.3837e-05s

3.1.5.3. Equation of State (EOS) Selection

The Mie–Grüneisen EOS was chosen for the copper liner due to its ability to describe the relationship between pressure, density, and internal energy in solid materials. It is derived from the Hugoniot relationships, which define thermodynamic properties across a shockwave. This makes it well-suited for simulations involving high-pressure states like those in jet formation [20].

An alternative such as the Ideal Gas EOS, is commonly used for explosive gases but is not suitable for solid materials. The Ideal Gas EOS assumes gas behaviour and cannot accurately model the response of solids.

3.1.5.4. Material Plasticity: Johnson-Cook Model

The Johnson-Cook plastic deformation model was applied to both the copper liner and the aluminium case. This model is suitable for capturing the effects of high strain rates, strain hardening, and thermal softening, which are essential during the collapse of the liner and the propagation of detonation waves. The Johnson-Cook model also accounts for temperature-dependent changes in material behaviour [21].

3.1.5.5. Omission of a Damage Model for the Case

The aluminium case was not assigned a damage model because it is not a primary focus of the simulation. The case is intended to propagate the pressure wave from the TNT explosive to the copper liner. Excluding the damage model provides two benefits:

- Solver Stability: Removing the need to calculate case fragmentation reduces the chances of solver failures.
- Faster Completion Time: Excluding case fragmentation reduces the solver's workload, meaning quicker simulation runs.

3.1.6. Mesh Validation

Effective meshing significantly influenced the outcomes of the simulations, impacting key parameters such as the accuracy of the jet formed, the jet velocity, the representation of high-stress and strain regions, and the overall simulation run time. The influence of meshing strategies on these factors was assessed through a series of simulations, utilising different seeding approaches.

3.1.6.1. Meshing Strategies

- General Seeding: Two simulations were performed using uniform general seeding across all components, including the liner, case and high-explosive (HE) fill.

- Targeted Local Seeding: Four additional simulations were conducted with a combination of general seeding for the case and HE fill plus local seeding in key deformation regions. These regions included (shown in Figure 6):
    - The centreline along the axis of symmetry, where high velocities and jet tip formation occur.
    - The liner edge, which experiences significant stress and strain during the collapse and jet formation process.

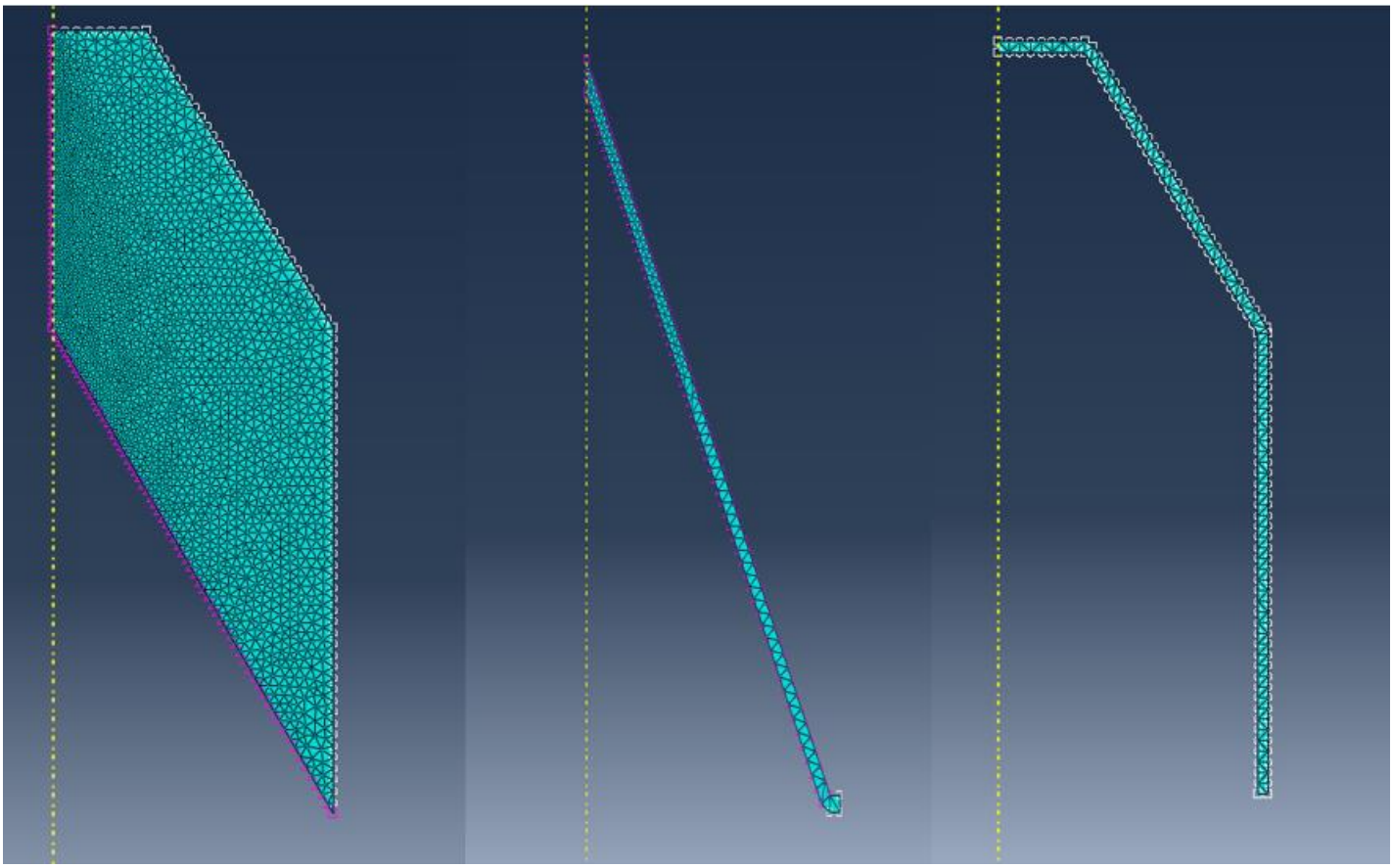

Figure 6 – use of local and general seeding

3.1.6.2.Meshing Results

Mesh Density	Run Time	Final time step	Peak Tip Velocity
0.001 Seeded 0.002 General	36s	9.8418E-05s	7km/s
0.002 Seeded 0.004 General	11s	1.0000E-04s	3.5km/s
0.004 Seeded 0.008 General	9s	1.0000E-04s	3.4km/s
0.0005 Seeded 0.002 General	116s	6.8119E-05s	6.8km/s
0.0005 general	756s	6.3837E-05s	7km/s
0.001 general	70s	9.0330E-05s	6.9km/s

Table 4 – Meshing Results

From table 4:

- Run Time: Seeded meshes resulted in significantly shorter run times compared to the corresponding general meshes, particularly for finer densities. For example, at 0.0005 density, the seeded configuration completed in 116 seconds, while the general mesh required 756 seconds.
- Final Time Step: Seeded meshes slightly increased the final time step in most cases, improving stability compared to general meshes.
- Accuracy: Finer seeded meshes (e.g., 0.001 Seeded / 0.002 General) captured higher peak tip velocities (7.0 km/s) and better resolved jet formation.
- Coarser meshes (e.g., 0.004 Seeded / 0.008 General) underestimated peak tip velocity, with lower accuracy in resolving jet dynamics.

3.1.6.3.Meshing results on jet formation

As mesh sizes decrease, the physical attributes of the jet become more accurate, as shown in Figures 7, 8, and 9.

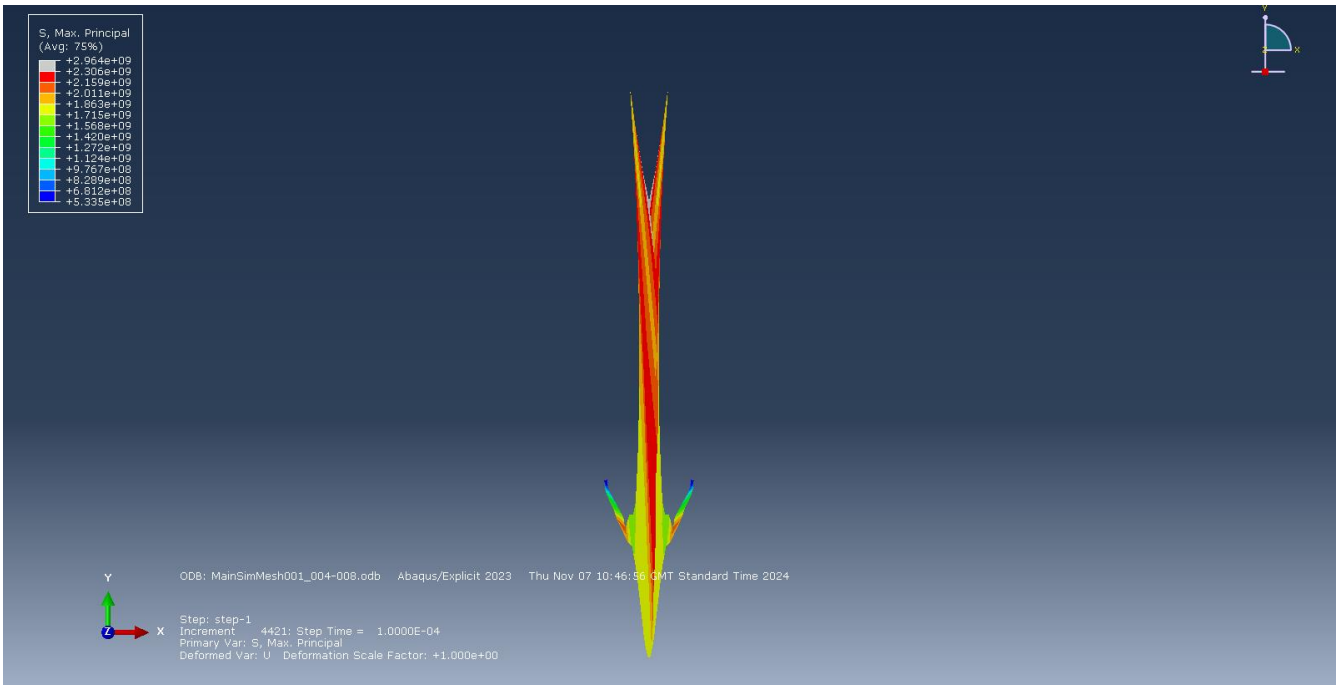

Figure 7 – jet formation of 0.004 Seeded / 0.008 general Mesh

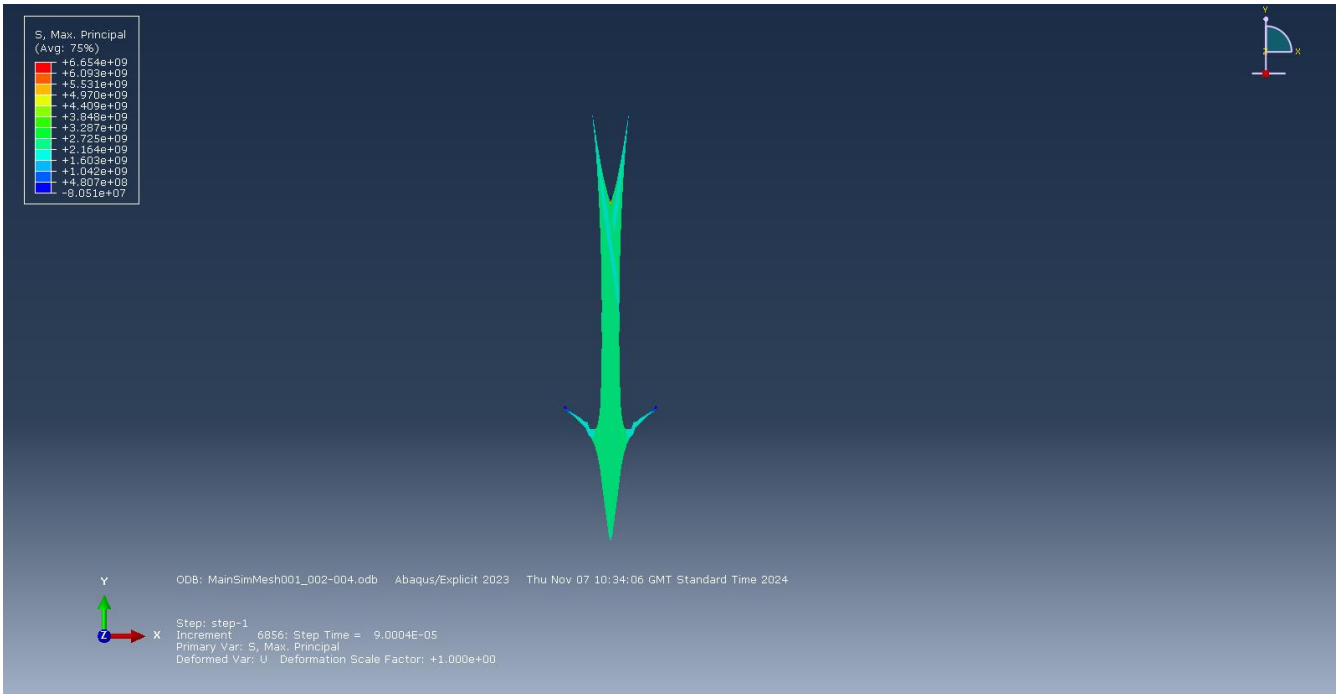

Figure 8 – jet formation of 0.002 Seeded / 0.004 general Mesh

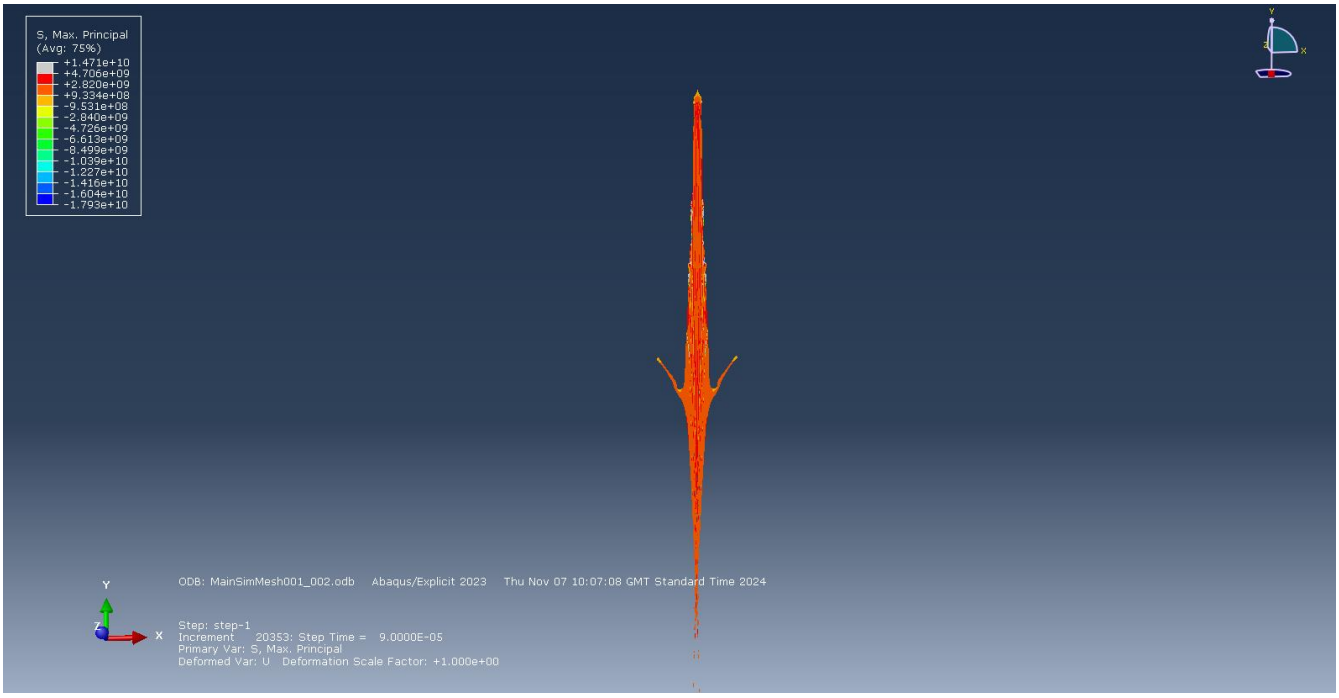

Figure 9 – jet formation of 0.001 Seeded / 0.002 general Mesh

The improvements in accuracy with decreasing mesh size are attributed to the increased number of nodes in finer meshes, allowing for more calculations per area. This shows a precise transfer of energy, better reflecting the physical behaviour of the jet.

In coarser mesh shown in Figure 7, inaccuracies in jet formation are evident. These include:

- A broader and less defined jet structure.
- Stress misrepresentations, where regions of high stress (highlighted in red) extend along the side of the slug to jet area. This distribution is inconsistent with jet formation theory, which predicts stress should concentrate around the forward body of the jet where the most significant deformation occurs.

- The twin tail is material being deformed in an inaccurate fashion where the HE fill is exerting force on the tip of the liner and splitting it rather than mostly travelling past this area.

In finer mesh shown in Figure 9, the jet formation more closely resembles theoretical expectations. The jet is narrower and more defined, with:

- Stress localised around the centreline of the jet, particularly near the forward body and tip the deformation is highest.
- A realistic transfer of energy from the explosive detonation to the liner material show by increased deformation.

For these reasons Figure 8 Is carried forward for Literature comparison.

3.1.7. Jet formation comparison

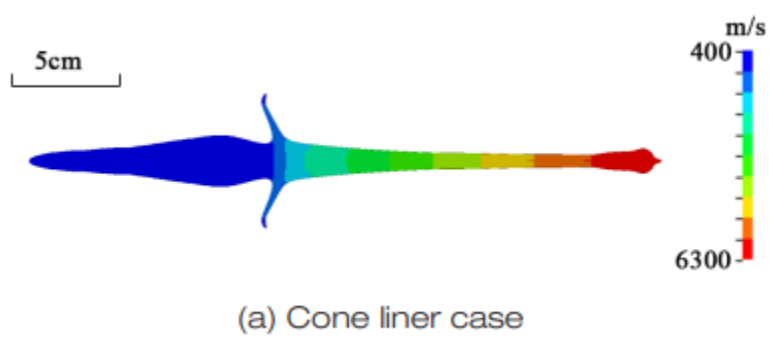

Figure 10 – Literature Jet formation at 6.9e-5s [14].

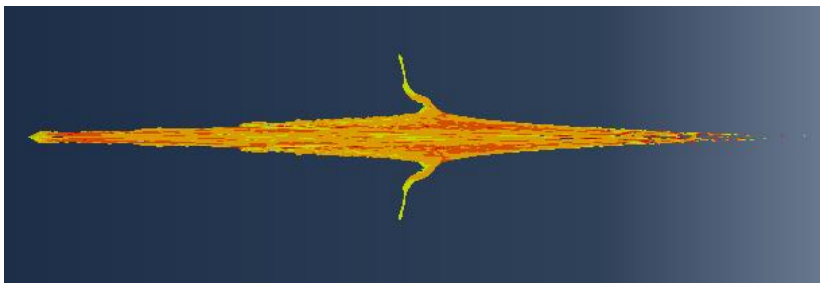

Figure 11 – Charge 1 Jet formation at 6.9e-5s

Figure 10 and Figure 11 demonstrate several similarities and key differences in jet formation characteristics.

3.1.7.1.Similarities

Material Distribution:

- Both simulations show a comparable distribution of material mass between the slug (area behind the conical plate) and the jet (area forward of the plate).
- The diameter of the plate area, formed by the outer edge of the liner, is also similar in comparison to the slug length, suggesting consistency in material flow during liner collapse.

General Jet and Slug Behaviour:

- The overall shape and segmentation of the liner into jet and slug regions exhibit alignment, reinforcing that the ABAQUS simulation produces results that are representative of known shaped charge behaviours.

3.1.7.2.Key Differences

Slug Material Behaviour:

- In Charge 1, some liner material moves backward during slug formation, resulting in a distorted slug shape. This backward movement occurs when the liner stretches in a direction opposite to the shockwave's travel direction.
- Cause: This is attributed to a calculation error in ABAQUS, where the furthest edge of the shockwave reflects backward during propagation, causing a portion of the liner to move in the opposite direction.
- Impact: While this behaviour affects the slug shape, it does not influence the forward jet's accuracy or the charge's penetration capability. The forward jet remains consistent with real-world performance expectations.

Forward Jet Shape:

- In Charge 1, the forward jet formation tapers to a sharp point, while in the literature simulation, the jet's tip exhibits a concentrated mass at the front.
    - ABAQUS uses a 2D simulation mirrored across the line of symmetry, which prevents the jet from extending beyond this axis.

- The literature simulation, however, models the jet in a 2D plane rotated 180 degrees about the ZX axis, capturing both sides of the jet more accurately.

These discrepancies do not significantly affect the accuracy of the jet's forward behaviour showing effective simulation of a shaped charge jet and coming to similar conclusions of jet formation as [14].

3.1.8. Jet tip Velocity at comparable time steps

Jet tip velocity shows whether energy has been accurately transferred between the HE fills and the Liner.

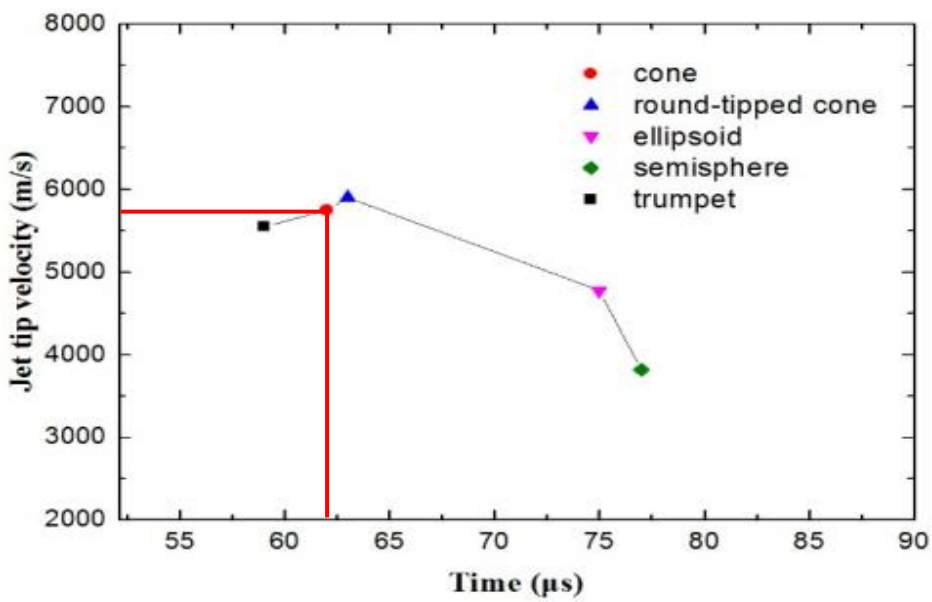

Figure 12 – Velocity over time literature charge [14].

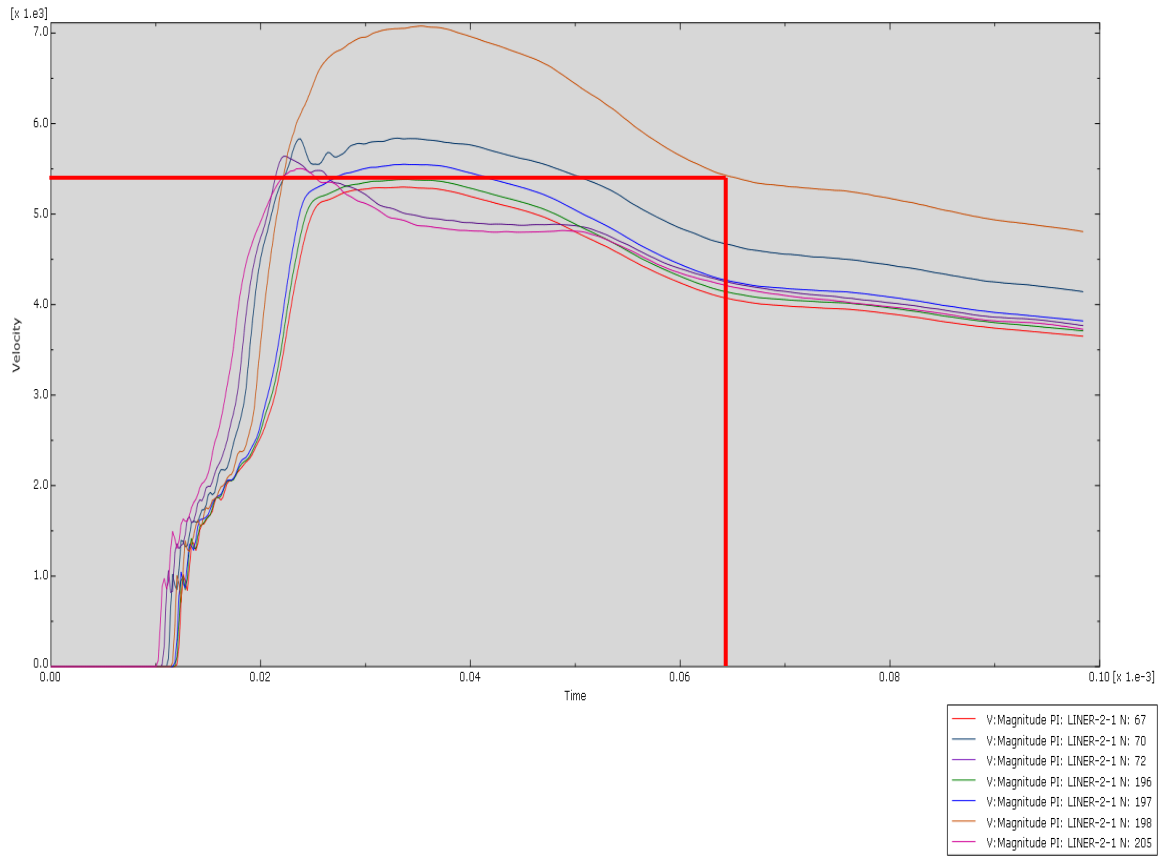

Figure 13 – Velocity over time charge 1.

The tip velocity of both charges (Charge 1 - 5.4×10^3 m/s, Literature Charge - 5.7×10^3 m/s at a time step of 64 microseconds) has a difference of approximately 5.26%. This demonstrates good accuracy between the two simulations, with relatively similar velocities at the same time step. The difference in these values could be attributed to variations in mesh densities and interactions causing differences in energy transfer between the HE and the liner. Additionally, the disparity may arise from the simulation methodologies, with the literature simulation using a 2D flat plane approach, while Charge 1 employs a mirrored half-plane simulation.

3.2.Jet formation theory

As illustrated in Figure 14, the tip of a shaped charge jet is formed from microelements located near the top of the liner. This region encompasses approximately the upper centre 1/4 of the liner near the apex. These microelements accumulate mass and are propelled forward during the detonation process, forming the leading tip of the jet.

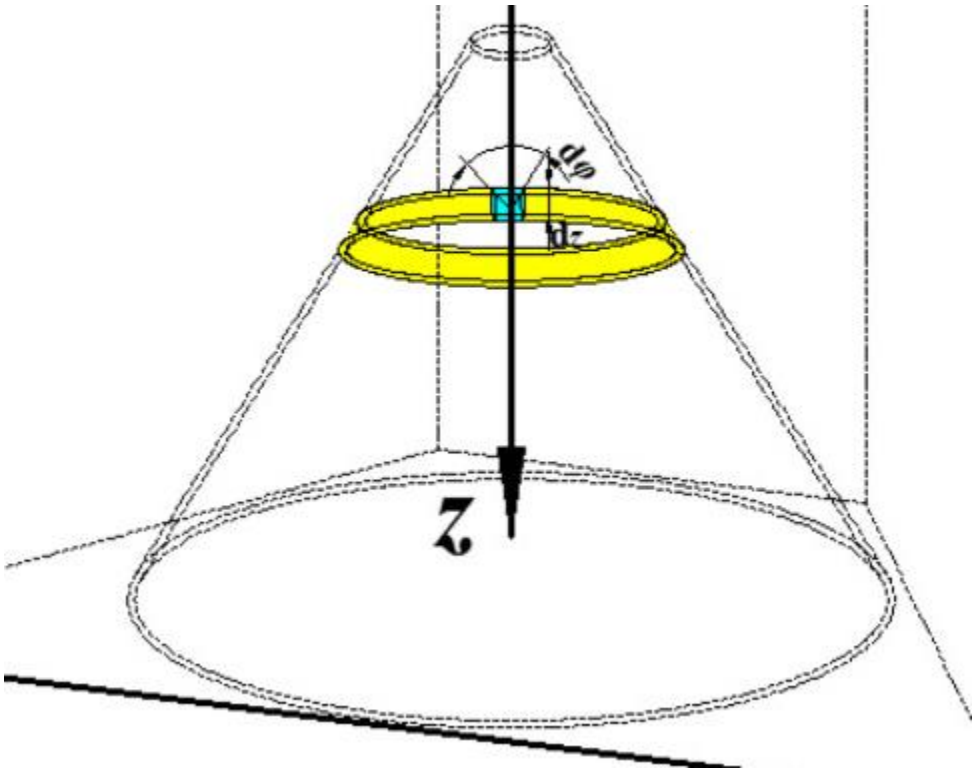

Figure 14 – Jet Tip formation zone [22]

This phenomenon is a direct result of the Munroe Effect, which describes the focusing of blast energy by a hollow or void on the surface of an explosive. As the liner deforms under the high-pressure conditions created by the detonation, the geometry of the deformation results in an increased flatter surface. This surface

provides an efficient area for the HE to transfer its energy, thereby accelerating the material in this specific region past the apex of the liner [1].

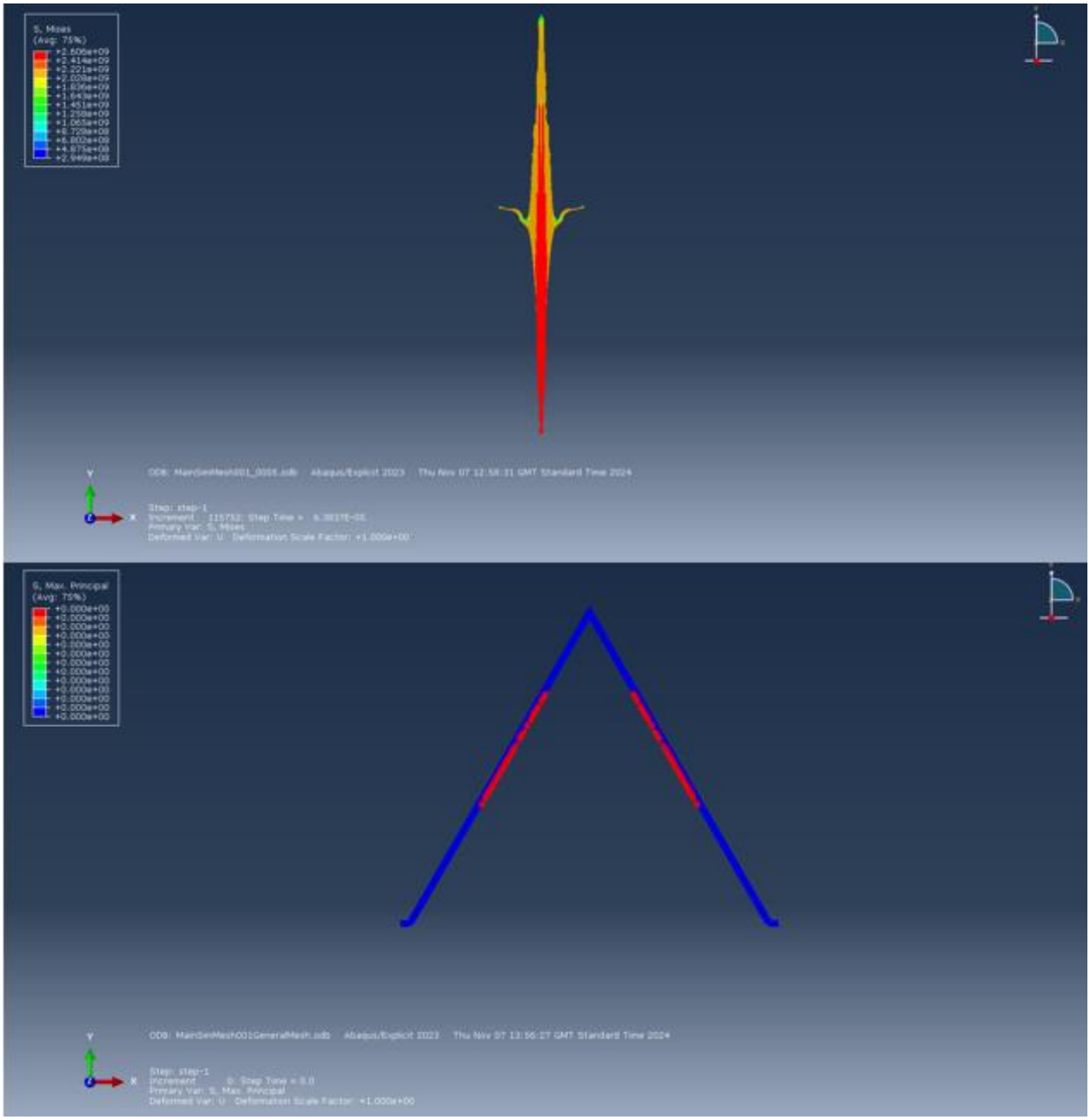

Figure 15 – charge 1 jet tip formation elements

The behaviour in Figure 15 aligns with this theory. The liner jet tip formation in the simulation accurately replicates the theoretical expectations, demonstrating the material acceleration that is characteristic of shaped charge jet formation. This

validates the reliability of the simulation in capturing jet dynamics driven by the Munroe Effect, with a caveat of some nodes stretching throughout a large amount of the slug-jet area.

3.3.Pressure wave propagation

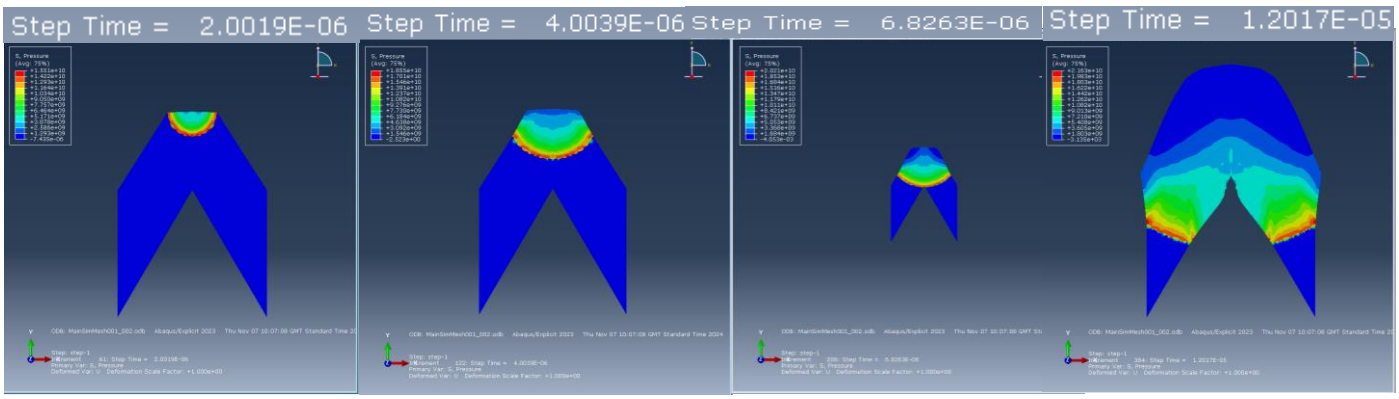

Figure 16 – pressure wave propagation in charge 1

Figure 16 demonstrates the accurate propagation of the pressure wave through the HE material. The wave originates uniformly from the initiation point and travels outward at a consistent velocity, maintaining a spherical detonation front. This symmetrical propagation ensures uniform energy transfer to the liner material, which deforms consistently along its surface [1]. The accurate representation of this behaviour proves model reliability for pressure fronts.

3.4.Validation Summary

The validation of the simulation results demonstrates an acceptable level of accuracy, with aspects such as jet formation, pressure wave propagation, and jet tip velocity aligning well with theoretical expectations and literature benchmarks. However, some caveats were identified, including node stretching in certain regions, which resulted in

deviations from accurate representations of jet tip generation theory. The meshing strategies employed were effective to a fair margin, though variations in jet formation were observed, including inaccuracies in the direction of slug formation due to shockwave reflections inherent in ABAQUS. Additionally, minor discrepancies in jet tip velocity (~5.26%) were noted, attributed to differences in mesh densities and simulation methodologies. Despite these limitations, the results provide a reliable basis for evaluating shaped charge jet dynamics.

4. 2D Shape charge with 120-degree Apex angle and Radius

A 2D model using a 120-degree apex angle and an apex radius was simulated (Figure 17), referred to as Charge 2. This model was developed in alignment with Section 2.2.5. These sensitivities can result in consistent failures when transitioning to 3D modelling.

Note: all other parameters are as per the validated model in 3.

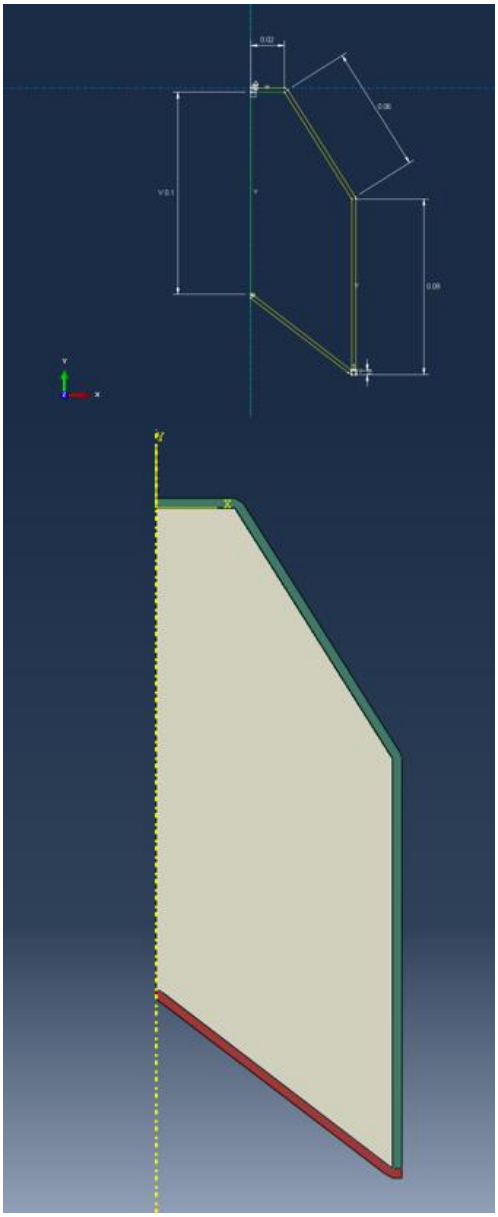

Figure 17 – 120-degree cone angle Shaped Charge

4.1.Liner Deformation

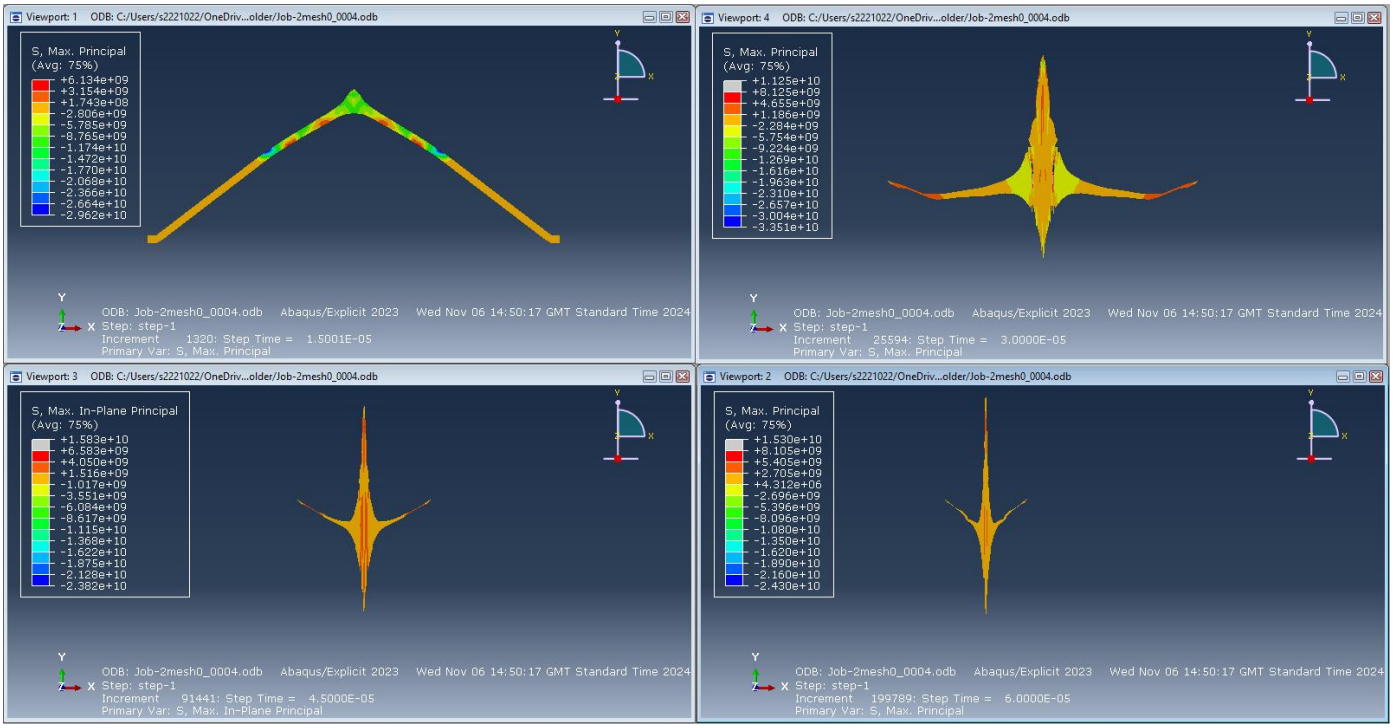

Figure 18 – charge 2 deformation

As shown in Figure 18, Charge 2 shows less deformation compared to Charge 1. This aligns with the expectation from 2.2.1, that a larger plate area is present in the final jet. The max principal stress is correctly shown in the high-deformation regions, with the material pushed from the apex experiencing elevated stress rates. This behaviour matches the expected material flow for a wider cone angle.

4.2.Jet tip Velocity

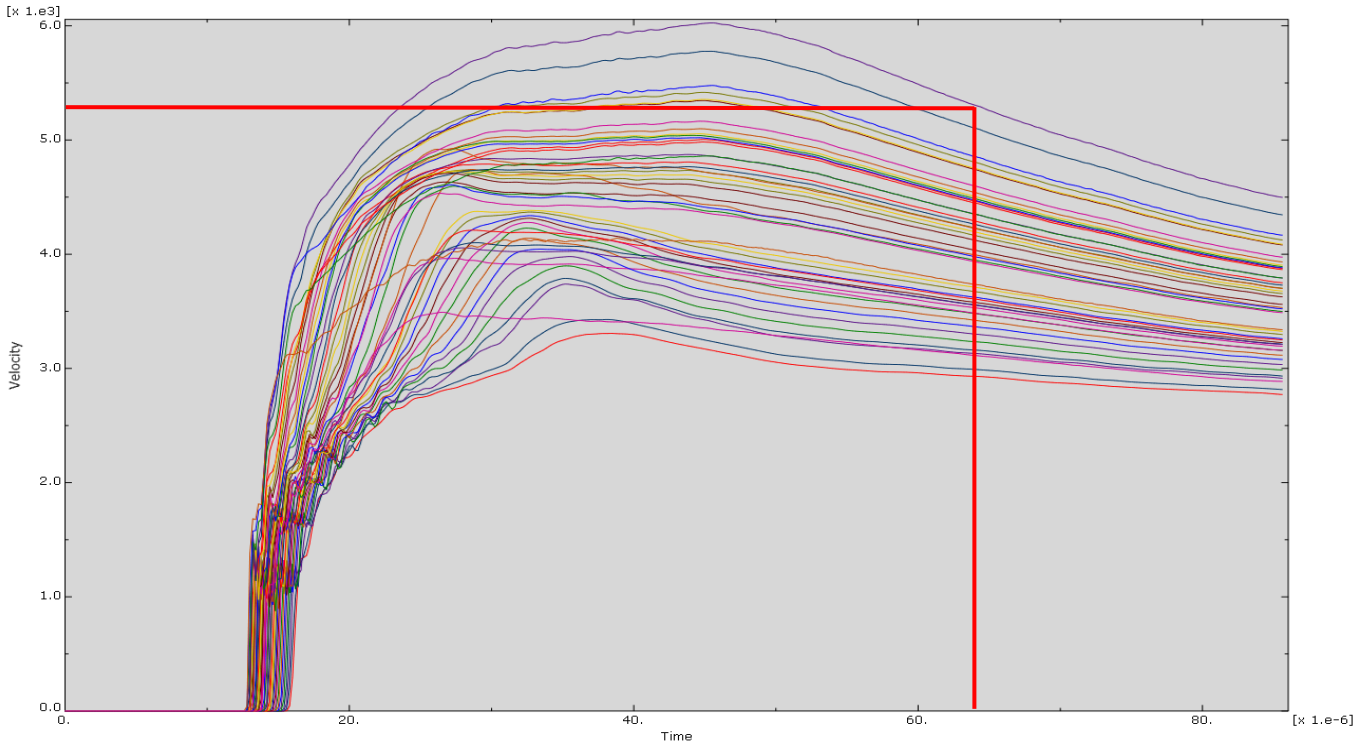

Figure 19 – charge 2 jet tip velocity

Figure 19, the jet tip velocity of Charge 2 is lower than that of Charge 1, as expected from Section 2.2.1. The peak velocity for Charge 2 is approximately 1 km/s lower than Charge 1 and at the same time step, charge 2 shows a velocity roughly 300 m/s lower. This reduction in velocity aligns with the wider apex angle of Charge 2, which results in a less concentrated energy transfer to the jet tip.

4.3.Pressure wave formation

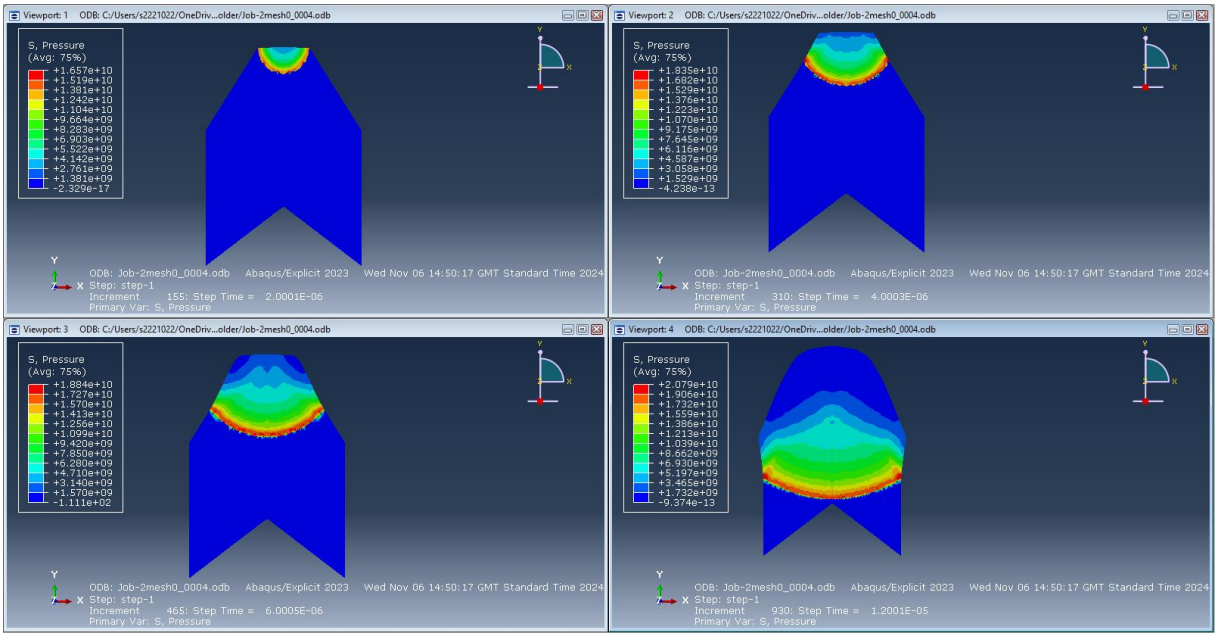

Figure 20 – Pressure wave formation charge 2

As shown in Figure 20, the pressure wave formation for Charge 2 propagates in a similar manner to the validation in Figure 16, with the highest-pressure areas located at the front of the shockwave. There is no liner interaction at identical time steps with Charge 2 as the cone angle causes larger distance between liner apex and point of detonation.

4.4.Overall

Charge 2 demonstrates key properties consistent with the validated liner model, including similar pressure wave propagation, stress distribution, and material flow dynamics. While some variations were observed, such as reduced liner interaction due to the larger apex angle, these align with theoretical expectations and do not compromise the model's reliability. The jet tip velocity and deformation also follow

expected trends for a wider cone angle. Therefore, Charge 2 can be considered an acceptable representation for use in a 3D modelling environment, with the same caveats outlined in Section 3.4

5. 3D modelling of charge 2

To build on the validated 2D model, the 3D simulation of Charge 2 was performed using the Lagrangian method, ensuring consistency with the earlier 2D work. General contact was defined between all components, allowing for automatic interaction handling without the need for explicitly defined contact pairs. This charge is referred to as Charge 3.

The 3D model was created to review the effects of the 3D domain on the high energy transfer scenario and evaluate what issues arise due to the element increase.

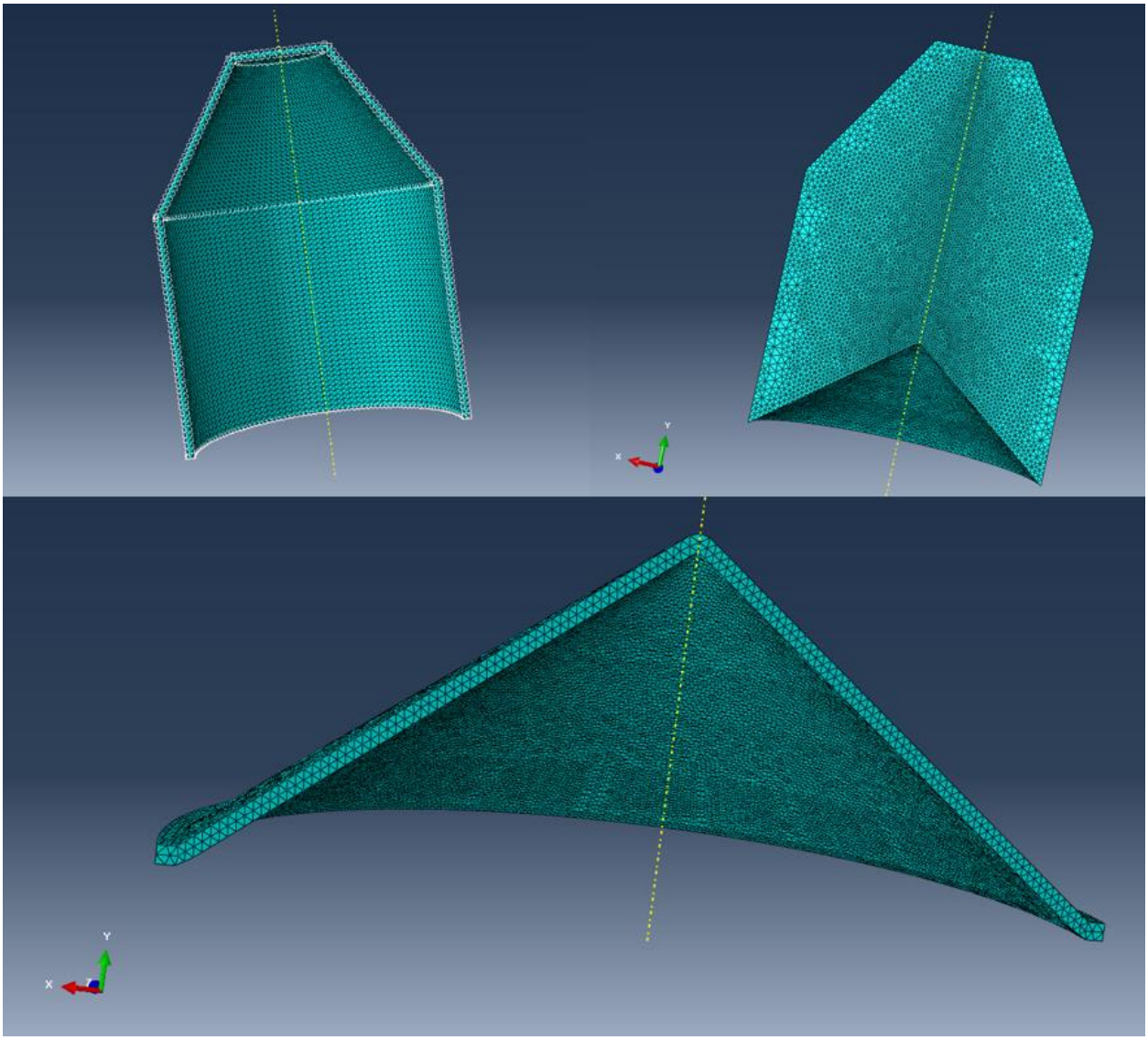

Figure 21 – Charge 3 parts

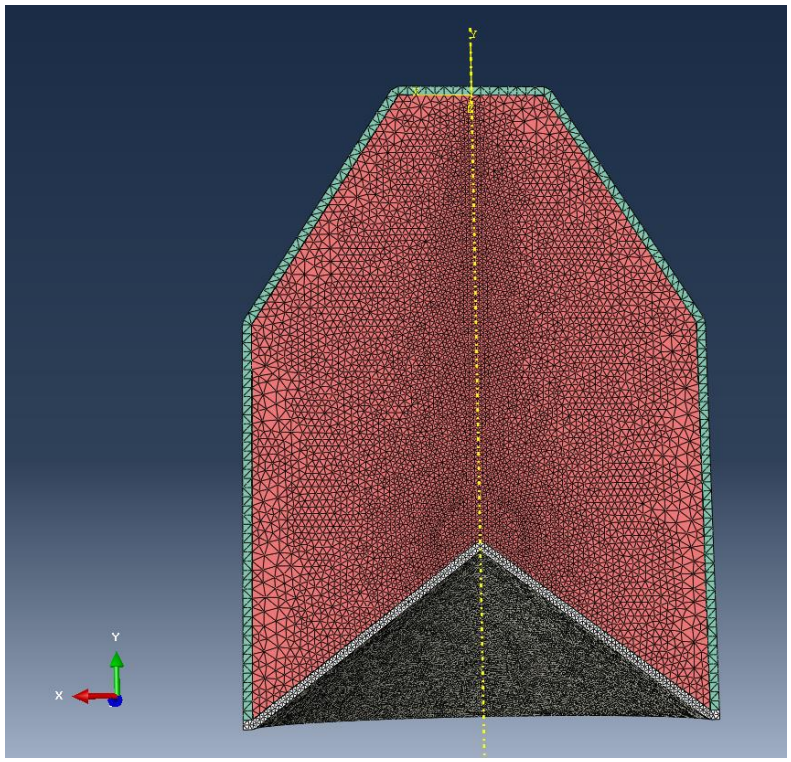

Figure 22 – charge 3 assembly

Figure 23 shows mesh validation, this is an easy way of seeing if nodes are likely to cause issue within the simulation (amber points are acceptable), due to this validation, mesh used as per Charge 2 is acceptable.

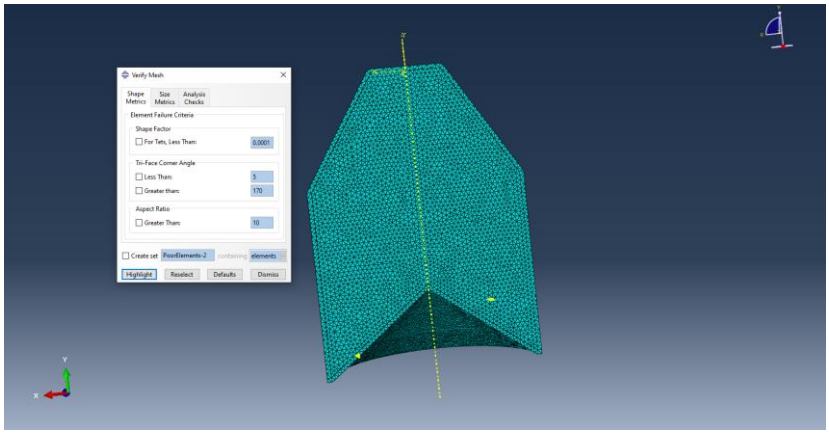

Figure 23 – Charge 3 Mesh validation

5.1.Initial results

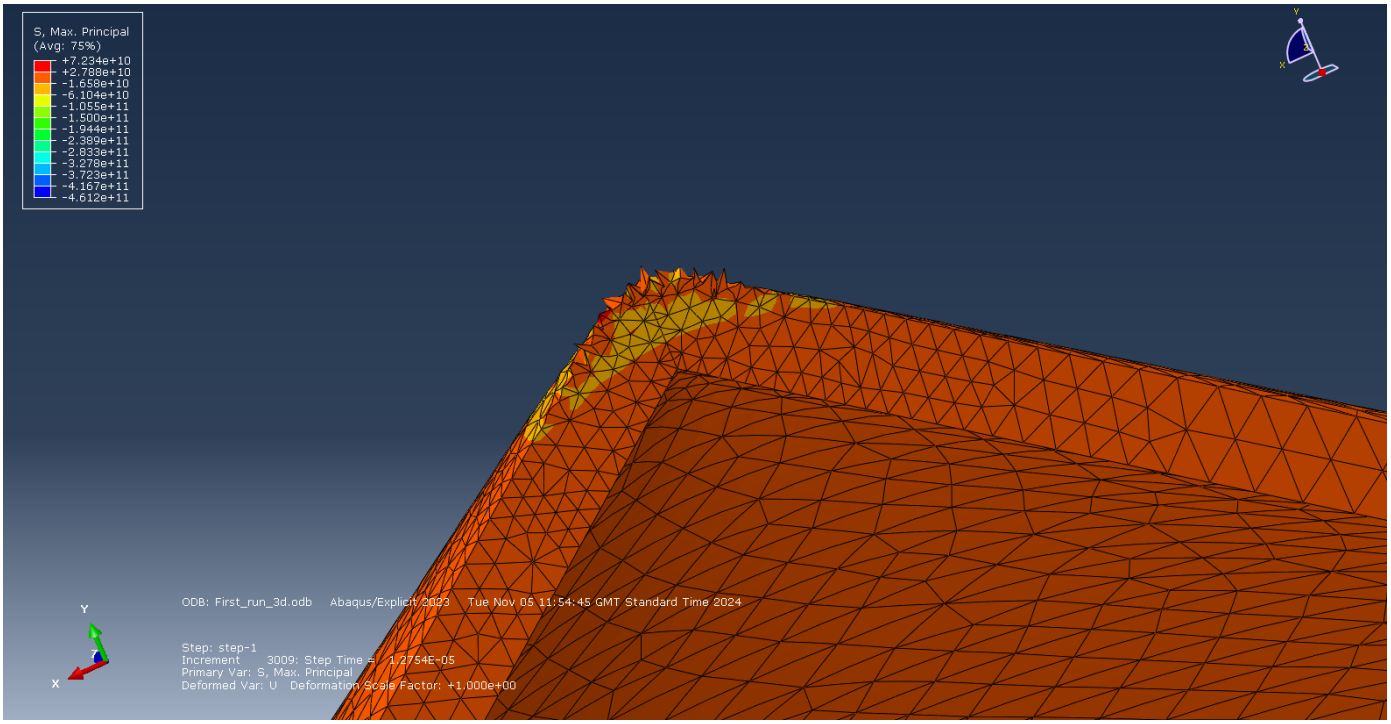

Figure 24 – initial liner Reaction, final time step

The initial 3D simulation failed at the point of energy transfer between the HE and the liner. Several elements distorted in directions inconsistent with the shockwave propagation and proper jet formation. This failure likely resulted from the increased number of nodes in the 3D space and the use of the Lagrangian method, which does not allow nodes to cross hard boundaries. While this feature is beneficial for simulating large deformations, the increased nodal interactions in 3D caused nodes to fail when crossing into neighbouring regions, leading to simulation failure. All validated variables were carried over from the stable 2D model, where a normalised jet was produced.

5.1.1. Resolution methodology

To address the failure of the initial 3D simulation, adaptive meshing and Smoothed Particle Hydrodynamics (SPH) were considered. Adaptive meshing was selected as it effectively manages large deformations while maintaining a stable mesh topology.

5.1.1.1.Smoothed Particle Hydrodynamics (SPH)

SPH is a Lagrangian method that discretizes continuum equations using points distributed over the solution domain, eliminating the need for a fixed spatial mesh. Its strength is handling large deformations and free surfaces naturally. However, SPH was unsuitable here:

- Works best in stable simulations, which was not the case.
- Represents materials as discrete particles, fragmenting the liner and preventing accurate jet formation, as shown in Figure 25.

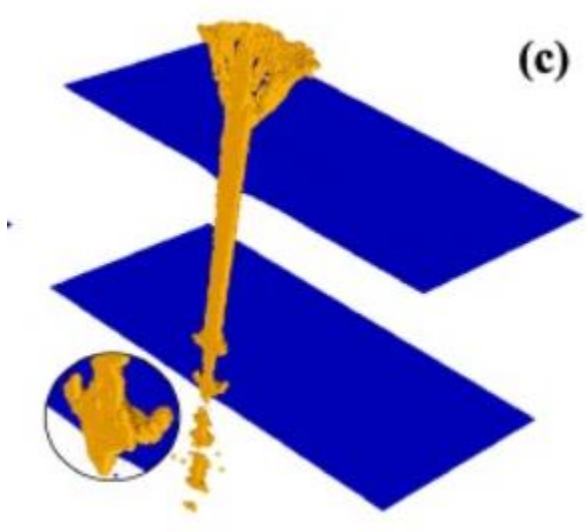

Figure 25 – SPH shape charge visualisation [23].

5.1.1.2.Adaptive meshing

Adaptive meshing performed using the ALE method generates a smoother mesh at regular intervals to reduce element distortion and maintain good element aspect ratios. This approach adjusts the mesh in regions with significant deformation while avoiding changes to the element topology [24]. Adaptive meshing was applied just before the failure point to minimise computational overhead in stable regions and ensure stability near critical areas, such as the liner and apex, as shown in Figure 26. This stabilised the simulation and allowed accurate jet formation.

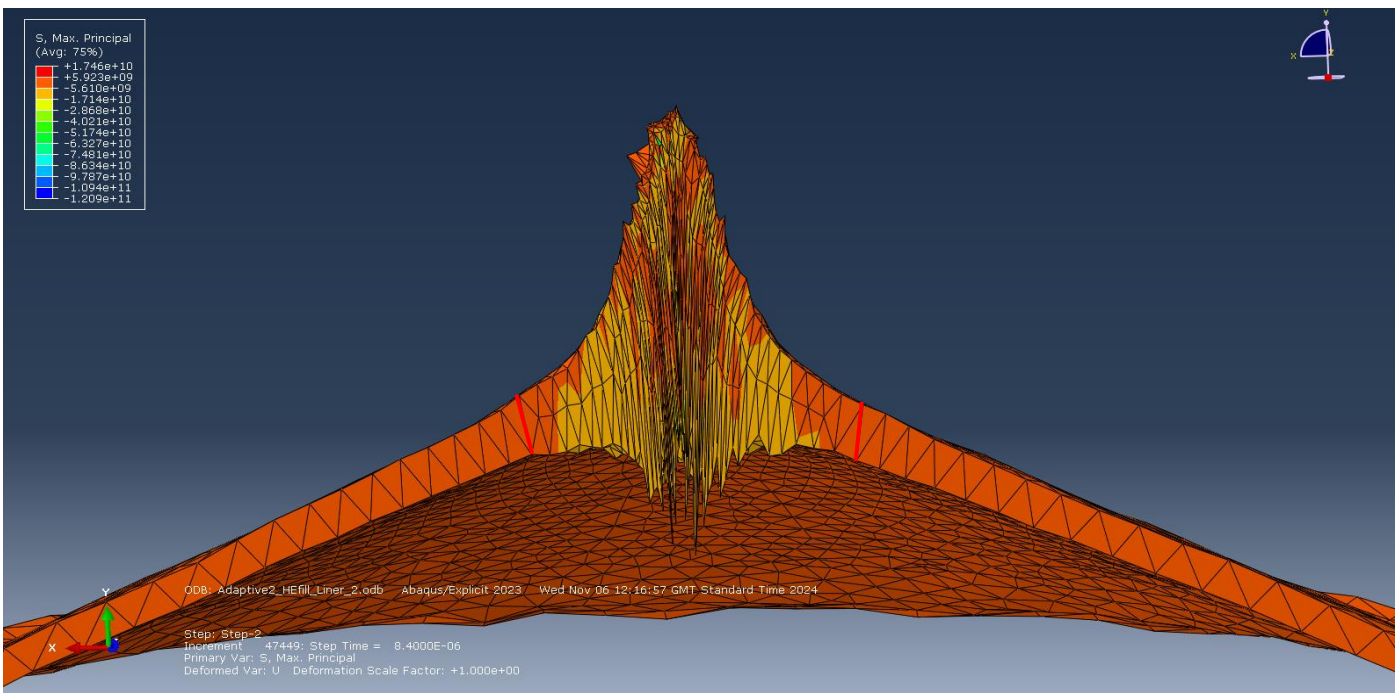

Figure 26 – Area for Adaptive Meshing + full run with secondary parameters

The use of adaptive meshing allowed for a 7-microsecond increase in the final step time, enabling a clearer review of the initial jet formation. While the jet shows some accurate behaviours, such as the compression of the apex into the initial slug, it also exhibits significant jagged elements that deviate from expected jet formation.

Initially, the linear and quadratic bulk viscosities were set to default values, which introduced minor rounding errors during the remeshing process, as shown in Figure 27. Bulk viscosity provides damping during volumetric straining. The quadratic bulk viscosity distributes the shock front across multiple elements, which reduces errors caused by high energy transfer but can also impact mesh accuracy. Increasing these values broadens the shock front and reduces the computational errors associated with rounding.

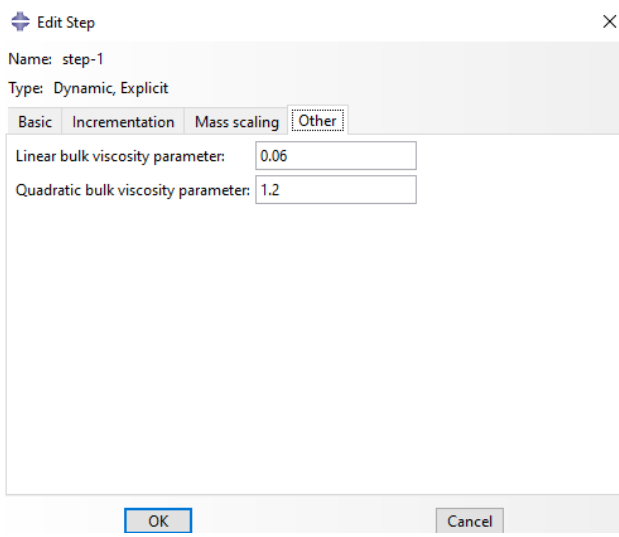

Figure 27 – Initial linear and quadratic viscosity parameters

To address this, the rounding margin was increased to a larger value (linear viscosity set to 1, quadratic viscosity to 10), as shown in Figure 28. Improving the stability of the remeshing process.

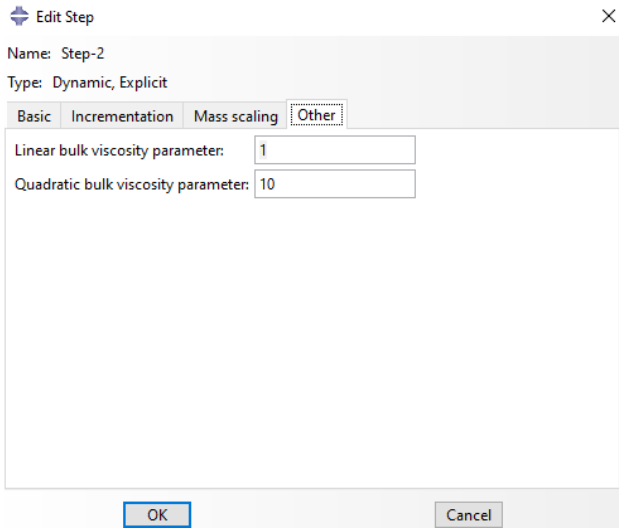

Figure 28 – adapted linear and quadratic viscosity parameters

The frequency and number of remeshing sweeps per increment were increased, ensuring remeshing occurred more frequently during each time step. This increased computational time but significantly reduced the failure rate by maintaining mesh quality by making smaller adjustments in smaller increments as shown in Figure 29.

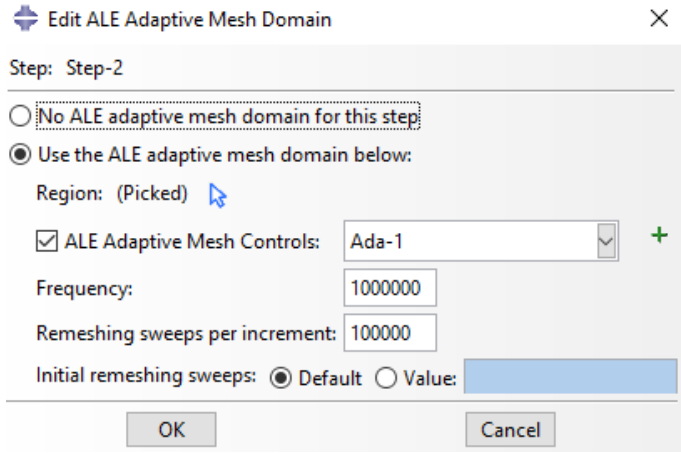

Figure 29 – Frequency of remeshing sweeps

Also volumetric, Laplacian, and equipotential weights control mesh quality during remeshing. Volumetric weight preserves element volume, Laplacian weight smooths the mesh by minimising distortion, and equipotential weight aligns the mesh with gradients

like stress or velocity. Due to the high distortion rates seen these were left as the default values (Figure 30).

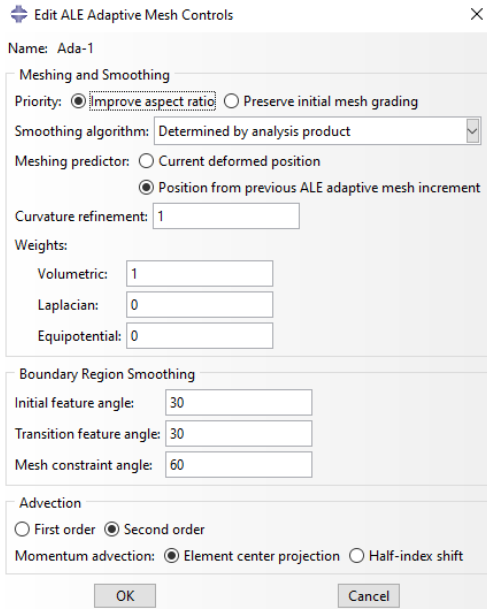

Figure 30 – Weight values

5.2.Final adaption results

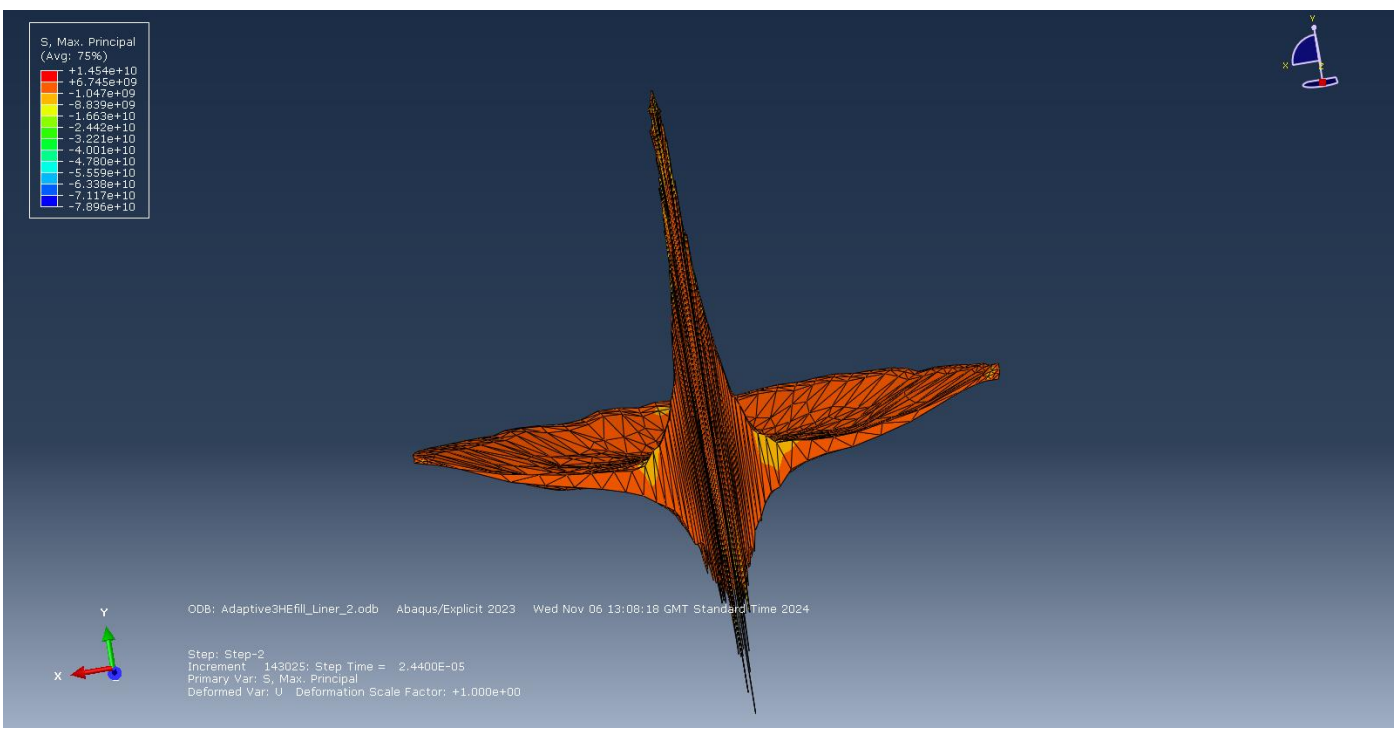

Figure 31 – Charge 3 final jet formation

With the adaptive meshing adjustments, the simulation ran to a duration six times longer than that shown in Figure 26, demonstrating a significant improvement in stability.

As shown in Figure 31, the jet formation follows the basic principles of jet formation theory, with material deforming to form a slug and jet. However, the material flow state, particularly the large amount of material forward of the liner, does not align with actual jet formation, as seen in Figure 32. This discrepancy is likely caused by overstretching of nodes, resulting from a non-uniform pressure wave interaction with the liner. These results highlight the impact of pressure distribution on accurate jet formation and indicate areas for further refinement.

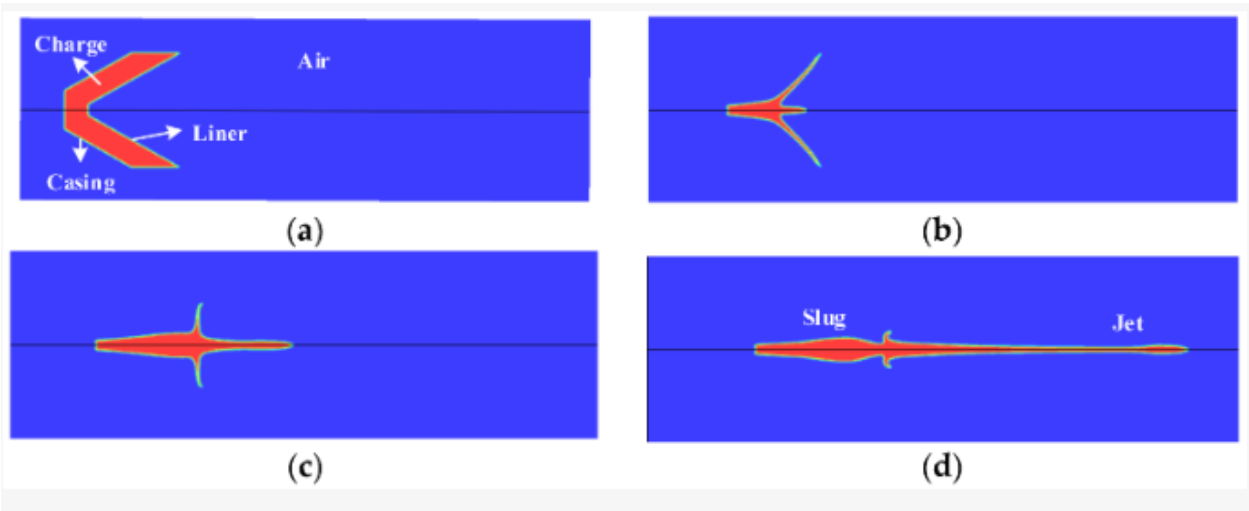

Figure 32 – Material deformation in jet formation [25].

As shown in Figure 33, the pressure wave within the HE propagates in the correct formation; however, the highest-pressure zone is not located at the front of the wave. This occurs because nodes at the leading edge are being interacted with earlier than expected due to the increased number of nodes. This behaviour does not accurately represent a

pressure wave, as the premature node interactions distort the expected progression of the wave front also causing dipped and spiked areas within the wave.

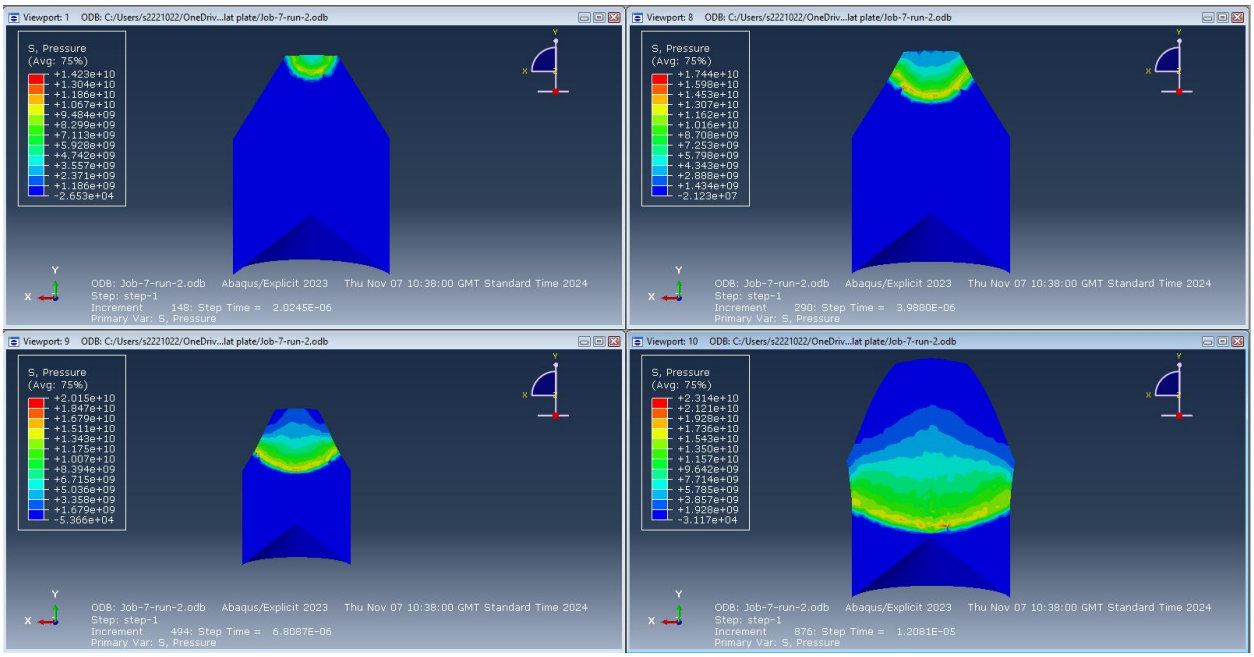

Figure 33 – Pressure wave propagation in HE, 3D

As shown in Figure 34, the jet velocity of Charge 3 is approximately 1.5 km/s slower than that of Charge 2, as seen in Figure 19. This deviation is a significant outlier compared to the expectations from the 2D validation and is identified as a notable anomaly. It indicates that the energy transfer between interacting surfaces is not occurring as expected, impacting the jet formation dynamics.

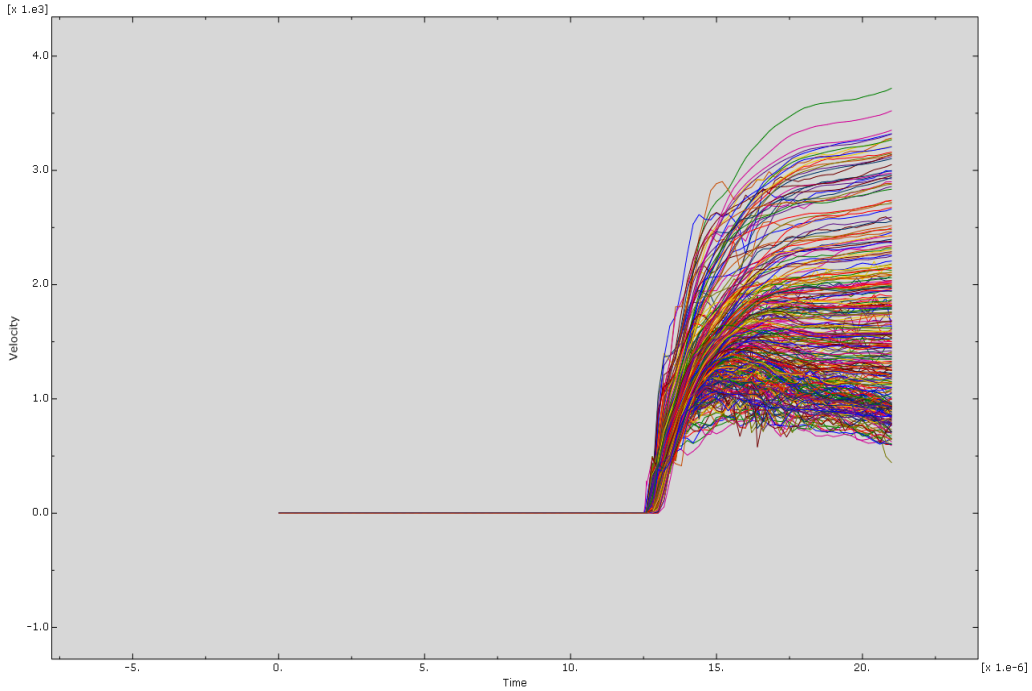

Figure 34 – Charge 3 jet tip velocity

6. Discussion

This study assessed ABAQUS's performance as an FEA tool for modeling shaped charge jet formation, transitioning from validated 2D simulations to more complex 3D environments. The 2D simulations demonstrated strong alignment with theoretical models and literature, accurately predicting jet velocities, pressure wave propagation, and material deformation. However, transitioning to 3D revealed challenges, including node overstretching, pressure wave distortions, and reduced jet velocities.

6.1.2D vs. 3D Simulations

The comparison between 2D and 3D simulations underscores the efficiency and reliability of 2D models for shaped charge design. 2D simulations effectively replicate key behaviours, such as jet formation and pressure wave dynamics, with significantly lower computational costs and reduced risk of instability. The

symmetrical nature of shaped charge designs aligns well with 2D modelling assumptions, making it an ideal approach for initial development.

In contrast, 3D simulations introduce complexities, including increased element counts, higher computational requirements, and greater potential for instability. While 3D modelling provides additional insights, such as asymmetries in jet formation, these details often do not justify the extra time and effort required. For most practical applications, 2D simulations are sufficient and should be prioritised, with 3D modelling reserved for cases where specific, detailed analysis is necessary.

6.2. Expected and Unexpected Results

The 2D simulations met expectations, with consistent jet formation, realistic pressure wave propagation, and velocities comparable to literature. These results validated ABAQUS's capabilities in predicting shaped charge dynamics. However, unexpected anomalies arose in 3D:

- Node Overstretching: Material forward of the liner deviated from expected jet formation due to non-uniform pressure wave interactions.
- Pressure Wave Distortions: Premature node interactions at the wave front introduced inaccuracies.
- Velocity Anomalies: Jet velocity for Charge 3 was 1.5 km/s lower than expected, indicating inefficient energy transfer.

6.3. Interpretation and comparison with theory

The 2D results align well with established theories, such as the Munroe Effect and the Gurney and PER models, confirming ABAQUS's effectiveness in modelling shaped charge jet formation in 2D. The discrepancies in 3D suggest challenges in translating these results, with mesh sensitivities and methodological constraints contributing to deviations.

The 3D anomalies highlight:

- Mesh Sensitivities: High element counts increased instability, especially during energy transfers.
- Simulation Constraints: The ALE method, while effective for adaptive meshing, struggled with uniform pressure wave propagation in 3D.

6.4. Generality and future Implications

These results emphasise the importance of prioritising 2D simulations in shaped charge design due to computation efficiency and alignment with theoretical expectations. While 3D modelling can provide additional insights, the complexities and computational demands often outweigh the benefits. Adaptive meshing improved 3D stability, but further refinements are needed to address node interactions and energy transfer anomalies.

Future work could explore:

- Testing alternative solver settings to address node overstretching.
- Refining adaptive meshing parameters to reduce anomalies.

- Integrating hybrid methods, such as SPH and ALE, for enhanced deformation handling.

7. Conclusion

FEA serves as a powerful tool for modelling shaped charge dynamics, offering a cost-effective and safer alternative to live testing during the initial design and evaluation stages. FEA can accurately simulate critical behaviours such as jet formation, pressure wave propagation, and material deformation, helping to anticipate the performance of a shaped charge. However, FEA should not be used in isolation. Without comparisons to validated literature or experimental data, there is no definitive way to prove the correctness, safety, or functionality of a shaped charge.

Literature provides the necessary theoretical background and benchmarks to ensure FEA simulations align with established principles and observed phenomena. By validating simulation results against previous studies, FEA can build confidence in its predictions while identifying areas for refinement. Despite its advantages, FEA cannot replicate the full complexity of real-world conditions, such as manufacturing imperfections or environmental factors, which are critical for ensuring safe initiation and accurate jet formation.

Therefore, FEA should be viewed as a complementary tool to live testing rather than a substitute. It is invaluable for anticipating shaped charge performance, reducing costs, and minimising risks during the design phase. However, live firing remains essential to

validate functionality under operational conditions and ensure safety before deployment. The integration of FEA with literature and live testing creates a robust framework for developing and assessing shaped charge designs.

Word Count – 5628 not including – Abstract, headers, Figures, Tables, Bibliography

8. Bibliography

[1 J. A. Z. William P. Walters, Fundamentals of Shaped Charges, J. Wiley, Ed., Maryland: A Wiley-Interscience Publication, 1989.

[2 D. Frem, "A mathematical model for estimating the Gurney velocity of chemical high explosives," *FirePhysChem,* vol. 3, no. 4, pp. 281-291, 27 09 2023.

[3 "A simple representation of the Pugh, Eichelberger, and Rostoker solution to the shaped charge jet formation problem," *Journal of Applied Physics,* vol. 50, no. 7, pp. 4667-4670, 01 07 1979.

[4 Z.-X. Zhang, Special Blasting Techniques, 2016, pp. 293-505.

[5 S. S. I Gokhan Aksoy, "Effect of the variation of conical liner apex angle and explosive ignition point on shaped charge jet formation," *Indian Journal of Engineering & Material Sciences,* vol. 10, pp. 381-389, 10 2003.

[6 G.-S. Yeom, “Numerical Simulation of Conical and Linear-Shaped ChargesUsing an Eulerian Elasto-Plastic Multi-Material Multi-PhaseFlow Model with Detonation,” *Materials,* vol. 15, no. 5, 2022.

[7 Y. J. Y. H. C. Han, “Study on the Penetration Performance of Microshaped Charge with Different Liner Materials,” *Journal of Physics: Conference Series,* 2021.

[8 NATO Standards, “AOP-4526 SHAPED CHARGE JET Munition Test Procedure,” NATO Standardization Office, 2018.

[9 “Theoretical Modelling of Shaped Charges in the Last Two Decades (1990-2010): A Review,” *Central European Journal of Energetic Materials,* vol. 9, no. 2, pp. 155-185, 2012.

[1 ADDNODE GROUP, “Abaqus/Explicit,” TECHNIA, [Online]. Available: https://www.technia.co.uk/software/simulia/abaqus/explicit/. [Accessed 5 11 2024].

[1 ANSYS AUTODYN, “How to model explosives in an ideal gas EOS?,” ANSYS AUTODYN, 25 01 2023. [Online]. Available: https://innovationspace.ansys.com/knowledge/forums/topic/how-to-model-explosives-in-an-ideal-gas-eos/#:~:text=You%20can%20model%20explosives%20in,used%20to%20model%20the%20explosives.. [Accessed 05 11 2024].

[1 S. Shlyk, “Research of ANSYS Autodyn capabilities in evaluating the landmine blast resistance of specialized armored vehicles”.

[1 E. GÜREL, “MODELING AND SIMULATION OF SHAPED CHARGES,” MIDDLE EAST TECHNICAL UNIVERSITY, 2009.

[1 J. Z. S. S. Z Liu, “Numerical Simulation on Conical Shaped,” *Int. Jnl. of Multiphysics,* vol. 13, no. 3, pp. 231-240, 2019.

[1 M. F. Z. A. ZHANG ZHIFAN, “NUMERICAL SIMULATION OF SHAPED CHARGE JET PENETRATING A PLATE USING SMOOTHED PARTICLE HYDRODYNAMICS,” Harbin, 2015.

[1 Y. M. B. S. V. L. S. V. Fedorov, “Numerical Analysis of the Effect of the Geometric Parameters of a Combined Shaped-Charge Liner on the Mass and Velocity of Explosively Formed Compact Elements,” *Combustion, Explosion, and Shock Waves,* vol. 51, no. 1, p. 132, 2015.

[1 B. M. Dobratz, LLNL Explosives Handbook, Livermore, California: lawrence livermore national laboratory, 1981.

[1 W. X. L. Z. W. L. Hossein Sedaghat, “on the constitutive models for ultra-high strain rate deformation of metals,” *International Journal of Automotive Technology,* vol. 20, no. 1, pp. 31-37, 2019.

[1 “Solid (continuum) elements - Abaqus Analysis User's Manual,” Abaqus, [Online]. Available:

https://classes.engineering.wustl.edu/2009/spring/mase5513/abaqus/docs/v6.6/books/usb/default.htm?startat=pt06ch22s01alm01.html. [Accessed 10 11 2024].

[2 A. C. Robinson, “The Mie-Grüneisen Power Equation of State,” Sandia National Laboratories, 05 2019. [Online]. Available: https://www.osti.gov/servlets/purl/1762624. [Accessed 10 11 2024].

[2 M. Veidth, “Introduction to Abaqus johnson-cook Model,” CAE Assistant, [Online]. Available: https://caeassistant.com/blog/abaqus-johnson-cook-model-video/#:~:text=The%20Johnson-Cook%20damage%20model,temperature%20effects%20on%20material%20damage. . [Accessed 10 11 2024].

[2 Z. H. Y. W. Y. W. X. J. G. G. Bin Ma, “Research on the Formation Characteristics of the Shaped Charge Jet from the Shaped Charge with a Trapezoid Cross-Section,” *Materials,* vol. 15, 28 10 2002.

[2 L. W. V. V. S. S. W. Zhifan Zhang, “SPH-FEM simulation of shaped-charge jet penetration into double hull: A comparison study for steel and SPS,” *Composite Structures,* vol. 155, pp. 135-144, 01 11 2016.

[2 “Defining ALE adaptive mesh domains in ABAQUS/Standard - ABAQUS Analysis User's Manual,” DSsimulia, [Online]. Available: https://classes.engineering.wustl.edu/2009/spring/mase5513/abaqus/docs/v6.6/books/usb/default.htm?startat=pt04ch12s02aus73.html. [Accessed 28 12 2024].

[2 S. L. S. o. S. C. P. a. C. Target, “Yi Zhang, Xiangru Zhang, Wenda Zhao, andFeng Hu,” *Buildings,* 17 11 2022.